ISSN 0915-633X

NATIONAL INSTITUTE FOR FUSION SCIENCE

The Role of Electric Field in Confinement

K. Itoh and Sanae-I. Itoh

(Received - July 27, 1995)

NIFS-366 July 1995

RESEARCH REPORT
NIFS Series

NAGOYA, JAPAN

The Role of Electric Field in Confinement

Kimitaka Itoh and Sanae-I. Itoh†

National Institute for Fusion Science, Nagoya, 464-01 Japan

† Research Institute for Applied Mechanics, Kyushu University 87, Kasuga 6-1, 816 Japan

Abstract

A review on the theories of the electric field effect on toroidal plasma confinement is presented. This review puts an emphasis on the recent progress in the area of the anomalous transport, structural formation and bifurcation, the research for which has been motivated by the finding of the improved confinement. Topics include the single particle physics, such as the particle orbit or the collisional transport, the turbulent transport, the transport matrix, the structural formation and dynamics, the bifurcation, and the improved confinement.

This article is prepared for a review in *Plasma Physics and Controlled Fusion.*

Keywords: Electric field, Particle orbit, Loss cone, Neoclassical transport, Turbulence, Anomalous transport, Structural formation, Improved Confinement

Contents

1. Introduction

More than a decade has past after the discovery of the H-mode [1]. The research of the plasma confinement has come to a new phase. This is also the case for the theory of confinement. This article tries to review the progress in this area of research.

The role of the electric field in confinement has been studied from the various aspects in the plasma physics and fusion research based on the toroidal confinement. Depending on the trend of the research, i.e., the particle trapping, the neoclassical transport, and the linear stability, a couple of reviews and text books have summarized the progress (see, e.g., [2-5]). The objective of this review article is to present recent progresses on this subject, which have been motivated by the finding of the H-mode [1] and various improved confinement modes, putting an emphasis on the possible future progress in the confinement physics.

In the beginning of the fusion research, the influence on the absolute trapping has been studied. The concept to confine plasmas by the radial electric field (i.e., through the $E \times B$ rotation) has been discussed [6] and this concept worked later in such a configuration like bumpy torus [7]. In the 60's, much work has been devoted to study the influence on the linear instability as well. The study on the particle orbit has been a subject of attention, when the theoretical method for the collisional transport was established as the neoclassical theory [8]. In the process of the collisional transport, the orbit deviation from the magnetic surface acts as a step size for the diffusion, so that the change of orbit was an important issue for the neoclassical transport. The effect of the electric field is most prominent for the particle which is trapped in the ripple of the main magnetic field (ripple trapped particles). The neoclassical transport was studied on stellarators (helical systems) intensively [9], associated with the high temperature experiment in helical systems. At the same time, the investigation in the mirror plasma, making use of the electric field effects, has flourished [10]. Since the particle motion parallel to the magnetic field is easily affected by the electric field, the concept such as

the tandem mirror was intensively developed [11]. In these researches, the aspect of the single particle dynamics was essential. The experimental study to realize the highest temperature plasmas was lead by tokamaks in this phase, and the anomalous transport was the dominant mechanism determining the plasma parameters [12]. (Status of the potential measurement is reviewed in [13].) The neoclassical theory and the single particle picture were not useful enough to understand these confinement. Partly because of the anomalous transport, and partly because the radial electric field was observed less frequently (compared to other plasma parameters) in tokamaks, the role of the radial electric field was not recognized much in these years.

As the H-mode has been found on ASDEX [1], the new phase of the confinement research started. The H-mode, which has short-cut the path in realizing the ignition by the enhanced confinement, has also given strong impact on the understanding of the nature of the confinement. It has revealed the fact that the steep gradient could be established (mainly near the edge in the beginning), the scale length of which seems to be independent of the plasma size: plasmas can sustain the self-organized scale length. The appearance of the H-mode is associated with the sudden transition (L-H transition) showing that the global plasma structure has a new time scale in addition to the usual one associated with the spatial diffusion. These two distinct features have excited the plasma physics. To understand these mysteries, the role of the electric field, which were not observed at the moment, was introduced. First, the role of the parallel electric field was investigated to explain the H-mode [14], although this idea turned out to be insufficient after the location of the steep pressure gradient was found experimentally inside of the plasma. Then the radial electric field was shown, theoretically, to cause the bifurcation and was proposed as the origin of the H-mode [15]. The existence of the radial electric field and its bifurcation were confirmed later by experiments [16]. Much stronger confidence to the tie between the radial electric field and the confinement was established, than the previous discussion based on the observation on stellarators [17]. Many theories on the H-mode were developed based on the concept of the radial electric field bifurcation (see, e.g., a review[18]).

Experiments have provided, one by one, new types of improved confinement mode, which further stimulated the theory of the radial electric field [19]. The study on the anomalous transport and the structural formation has come to a new stage along this line of thought.

These theoretical development and the future trend are the main subject of this article, which would be complementing previous reviews on electric field problems (e.g., reviews [2-5,10,20]). This article is organized as follows. In order to clarify the role of the radial electric field in the confinement, we take the view point shown in Fig.1. In the first step, the response of the plasma to the electric filed is discussed. In explaining this process, the electric field is treated as a parameter, and the reactions of the plasma are shown. Next, the mechanism of the formation of the radial electric field is explained. Then a closed set of plasma equations, which tries to consistently describe the structures of the plasma and electromagnetic field, is constructed. The theoretical results out of this set of equations are described, and the relations with the improved confinement modes are discussed. Status of the comparison with experiments is surveyed, in order to identify the theoretical problems. Summary and future prospect are finally presented.

There are several limitations in the scope of this article, and references may not be exhaustive. First, majority of the article is devoted to the dynamics governed by the electrons and main ions; Studies on the impurities, neutral particles and plasma wall interactions are interesting area in analyzing the role of electric field, but only few is discussed. The electric field structure along the field line is also an important subject, but is not included. Related to this, the topics of the electric field in the scrape-off layer (SoL) plasma is not covered. Discussion on the linear stability theory is limited as well. This is partly because of the length limitation; although the linear stability provides the useful information on the possible free energy source for the plasma dynamics, but nevertheless, its applicability to understand the dynamics and fluctuations is fairly limited. Emphasis is made on the analytic insight of the problem.

2. Effect on the Particle Orbit

We first briefly discuss the effect of the radial electric field on the single particle orbit. Figure 2 illustrates the model geometry in the analysis. Coordinates (r,θ,ζ) and (R, ζ, Z) are used for toroidal plasmas. When the cylindrical model or slab model are employed, coordinates (r,θ,z) and (x,y,z) are used, respectively, as is shown in Fig.2. Magnetic surfaces are considered to be nested, unless specified otherwise, and is labeled by the coordinate r, or x. Plasma cross section is characterized by the minor radius a and the major radius R.

The trapped particles exist due to the field inhomogeneity. The toroidicity gives rise to the trapped particles (banana particles)which are localized near the low field side (outside) of the torus. Toroidal coils and helical coils generate other kind of trapped particles: the ripple trapped particle. The orbit of the ripple trapped particles are schematically illustrated in Fig.3.

2.1 Drift and Resonance

The trajectory of the trapped particles are influenced strongly by the radial electric field. The influence is most prominent for the ripple trapped particles. The banana orbit could also be modified, if E_r becomes strong enough. (In principle, the gyro motion itself could change its character, but is not discussed here.)

The motion of the ripple trapped particles is described by the three elements, i.e., (i) gyro-motion, (ii) bounce motion of the guiding center (i.e., banana orbit) and (iii) drift of the center of the banana. These elements constitute the deviation of the particle orbit from the magnetic surface. In usual situations the last one has the largest contribution. The influence of the radial electric field is noticeable if the potential change during the bounce motion (say banana or drift of ripple) is a considerable fraction of the particle kinetic energy. Because the drift motion, (iii), has the largest excursion in radius, it is most vulnerable to the radial electric field. If the influence of

the electric field is so large that the orbit is strongly changed, we use the term *'resonance'*.

The motion of the ripple trapped particles in toroidal ripples (that in tokamaks) is limited by the two adjacent coils. The motion of the banana center is expressed in terms of the drift motion, v_G, as [2]

$$v_G = v_D\hat{Z} + \frac{E_r}{B}\hat{\theta} \tag{1}$$

where v_D is the drift by the toroidal field inhomogeneity, $v_D \approx W/eBR_m$, where W is the particle energy, B is the main magnetic field and R_m is the scale length of toroidal field inhomogeneity. (For the transparency of the analytic insight, a simple relation $R_m \approx R$ is employed in this article unless specified otherwise.)

This result shows that the motion of the ripple trapped particle is determined by the combination of the vertical drift and the poloidal drift. It could be possible that the poloidal rotation dominates over the magnetic drift, and ripple trapped particle turns to the banana particle. The trajectory on the poloidal cross section (R,Z) of the particle, which started from the initial condition (R_1, Z_1, κ_1), is given by the integral of motion W and μ (magnetic moment) as

$$\Psi_0(R,Z) + \frac{R}{R_0} - 1 = 1 - \frac{W}{\mu B_0} \tag{2-1}$$

$$\Psi_0(R,Z) = \left\{\sqrt{\varepsilon_r(R,Z)} - \kappa_1^2\sqrt{\varepsilon_r(R_1,Z_1)}\right\}^2 - \kappa_1^4\varepsilon_r(R_1,Z_1) - \frac{e\phi}{\mu B_0} \tag{2-2}$$

with $\kappa^2 = \{W - \mu B_0(R_0/R - \varepsilon_r) - e\phi\}/(2\varepsilon_r\mu B_0)$ denoting the pitch-angle, B_0 is the main magnetic field, ε_r is the amplitude of the ripple, ϕ is the static potential, e is the charge (notation is used after [21]).

This formula provides the estimate of the shift in the major radius direction, as the ripple trapped particle moves in the vertical direction. This result also shows the

dispersion of this shift, depending on the pitch angle; the value κ takes the number in between 0 and 1.

Consider the case where radial electric field of E_r exists in the region of thickness Δ. If the poloidal rotation is large enough,

$$|\Delta e E_r R/aW_\perp| \approx 1, \tag{3}$$

the particle moves in the poloidal location where the toroidal ripple is weak. This relation gives an estimate for the detrapping of the ripple trapped particle.

The fraction of the ripple trapped particle is of the order of $\sqrt{2\varepsilon_r}$. Although the number of the ripple particles is very small, the influence could be important, because these processes appear for energetic particles (associated with intense heating or the fusion product) and are localized in space [22].

Similar description is available for the motion in the helical trapped particles in the helical systems, by replacing ε_r by the helical ripple, ε_h. Leaving detailed argument, which corresponds to Eq.(2), to literature [4, 23], qualitative explanation is given here. The main difference is that, in helical devices, ε_h could be as large as, or more than, the toroidicity $\varepsilon_t = r/R$. (The toroidicity ε_t is abbreviated by ε for the simplicity). Considerable part of the particles are within this category, and it could be essential in the transport. The gradient of the magnetic field, which helical ripple trapped particles feel, is ε_h/r, and the curvature directs in the radial direction. The drift velocity is given as

$$v_G \simeq v_D \hat{Z} + \left(\frac{W\varepsilon_h}{eBr} + \frac{E_r}{B}\right)\hat{\theta} \tag{4}$$

showing that the banana center rotates in the poloidal direction with the angular frequency

$$\omega_{rot} \simeq r^{-1}\left(\frac{W\varepsilon_h}{eBr} + \frac{E_r}{B}\right) \tag{5}$$

as is schematically shown in Fig.3 [2]. The deviation of the banana center from the average magnetic surface, ρ_{heli}, is given by v_D/ω_{rot}, or

$$\rho_{heli} \simeq \frac{r^2}{\varepsilon_h R} \frac{1}{(1 + erE_r/\varepsilon_h W)} . \qquad (6)$$

Two characteristics are seen in this simple but useful result. First, the deviation ρ_{heli} is a function of, dominantly, the geometrical factors (R, r, ε_h) and is independent of the magnetic field. As a result of this, ρ_{heli} is of the order of system size, rather than to scale with the gyro-radius or banana width. Second, the ratio $erE_r/W\varepsilon_h$ plays the essential role in characterizing the orbit. If it satisfies the condition,

$$\frac{erE_r}{\varepsilon_h W} \sim -1$$

the poloidal rotation Eq.(5) cancels, and the shift becomes very large. It is called as the resonance of the ripple trapped particle, and can lead various dynamic phenomena.

The resonance condition is sign dependent. If the charge is positive (i.e., ions), the resonance occurs when E_r is negative. In opposite case ($E_r > 0$), it occurs for the electron orbit. The situation of the negative electric field corresponds to the case where electrons are rich; In other words, there is a mechanism for the selective loss of ions (such as via hot ion loss). The loss of ions which precedes electron loss, makes the negative radial electric field and gives rise to the resonance on the ion orbit. (The same situation holds for electrons if $E_r > 0$). The dependence of the resonance condition on the sign of the electric field gives the mechanism for the self-sustaining of the electric field, which will be discussed later.

Banana orbit itself is influenced by the strong radial electric field. Due to the E× B motion, trapped particles (those which is trapped in the toroidicity, not in ripples) drift in the toroidal direction with the velocity of E_r/B_p. This velocity is associated with the centrifugal force, and is reflected in the bounce motion as well. The parallel

velocity and the deviation of the guiding center from the mean magnetic surface is given as [24]

$$u_{\parallel}^2 = u_{\parallel 0}^2 - \varepsilon(1-\cos\theta)(u_{\perp 0}^2 + 2u_E^2) + u_g\delta^2 \tag{7-1}$$

$$\delta = (u_{\parallel 0} - u_{\parallel})(1 - \varepsilon\Lambda\cos\theta) + 2\varepsilon(1-\cos\theta)u_E \tag{7-2}$$

where $u = v/v_{th}$,

$$u_E = E_r / B_p v_{th} \tag{8-1}$$

and

$$u_g = \rho_p (dE_r/dr)/B_p v_{th}. \tag{8-2}$$

are normalized velocities, Λ is the Shafranov Λ [2] in this equation, δ is the deviation normalized to poloidal gyro radius, and the suffix 0 denotes the poloidal location $\theta = 0$. From this relation, one sees that the boundary between the trapped and transit particles are deformed as

$$u_{\parallel 0}^2 = \varepsilon(1-\cos\theta_b)(u_{\perp 0}^2 + u_E^2) \tag{9}$$

where θ_b denotes the poloidal location of the banana tip. The boundary is now given by the hyperbola as is shown in Fig.4. The bounce frequency is up-shifted as

$$\omega_b = \sqrt{\varepsilon/2}(v_{th}/qR)\sqrt{u_{\perp 0}^2 + u_E^2}\ .$$

Since the E× B drift is common for the electrons and ions, the parameters u_E and u_g are much smaller for electrons. In the following, these parameters are used for ions.

2.2 Orbit Squeezing and Drift Reversal by Inhomogeneous Radial Electric Field

In the presence of the strong radial electric field, such that the banana orbit is influenced, the role of the inhomogeneous radial electric field becomes important as well [24,25]. The maximum value of the radial motion δ can be compressed or enlarged. The effective poloidal gyro-radius is given as [25]

$$\hat{\rho}_p = \rho_p / S \tag{10}$$

where ρ_p is the usual poloidal gyro-radius, and S is the squeezing parameter defined as

$$S = 1 - u_g \, . \tag{11}$$

If the parameter S is greater than unity, i.e., dE_r/dr is negative, the banana width is compressed. Notice that there is also the resonance condition, $u_g \approx 1$, for which the banana orbits expand greatly.

The toroidal precession velocity of trapped particles is also affected. It was given as [26]

$$v_{D,t} = -\left(1 + 2u_g\right)\frac{W_{\perp 0}}{reB_p} \, . \tag{12}$$

This result shows that, if dE_r/dr is negative, the drift of the trapped particle in the bad curvature is reduced. When the electric field inhomogeneity is large enough such that the condition $1+2u_g < 0$ or

$$u_g < -1/2 \tag{13}$$

is satisfied, the drift of the trapped particles directs in the opposite direction: Trapped particles drifts as if it were in the good curvature. This situation is called as the *drift reversal* and has influence on the plasma stability and transport. (Note that the E×B drift is charge independent, while this drift due to E_r' depends on the charge. The latter can influence on the stability in the first order, while the former affects in the second order.)

2.3 Loss Cone

The loss cone of the particle is also influenced by the radial electric field or its inhomogeneity.

As the trapped-transit boundary is deformed in the phase space, the loss cone boundary is modified by the radial electric field as is shown in Fig.4. This is the case of the poloidal limiter at $\theta = \theta_b$. The number of particles at the tip of the low-energy boundary of the loss cone in the phase space is reduced by such a factor like $\exp(-u_E^2)$ if the distribution is given by the Maxwellian.

In the presence of the separatrix at the surface, the separatrix of the drift surface appears [27]. The loss boundary becomes narrower as the radial electric field becomes strong enough. Reference [27] claims the asymmetry with respect to the sign of E_r: the loss region first slightly increases as it becomes negative. No asymmetry is found about the direction of the gradient-B drift with respect to the direction of the x-point of the separatrix magnetic surface.

Due to the large deviation, the ripple-trapped particles easily reach the plasma surface. For the clarity of the argument, we define the loss cone boundary for the trajectory touching the plasma surface. (One could choose other definitions, such the surface of device.) The boundary in the radial-energy space is given in literature [4,23,28]. Simplified expression for the case of the monotonic potential $\phi(r)$ is given as

$$W_+ < W < W_- \tag{14-1}$$

with

$$W_\pm = \frac{e\{\phi(a)-\phi(r)\}}{\varepsilon_h(a)(1-r^2/a^2)\pm(a/R)(1-r/a)} . \tag{14-2}$$

This expression is derived for the particles which are deeply trapped in helical ripples. The region of the loss cone in the phase space is shown in Fig.5. For the potential difference of the order of

$$\phi(a)-\phi(0) \approx \varepsilon_h(a)W/e,$$

the loss cone of ions spreads over the plasma column. A wide loss cone appears for electrons for the opposite sign of the electric field.

3. Collisional Transport (Neoclassical Transport)

The modification of the orbit by the radial electric field affects the collisional transport. In a dimensional argument, the collisional (neoclassical) transport coefficient depends like $D \sim \nu_{eff}\delta^2$, where ν_{eff} is the Coulomb collision frequency for the relevant particles contributing the transport. The deviation of the orbit from the magnetic surface, δ, is subject to a strong change. It should be noted that care is necessary for the collision frequency as well. Microscopic origin of the Coulomb collision is the thermal fluctuation in the range of the electron plasma frequency [29]. The thermal fluctuation, defined in the absence of inhomogeneity, may not be changed by the electric field of the present interest. However, the energy of the relevant particles changes in the phase space, as is shown in Figs.4 and 5. Therefore the effective collision frequency can change, if it is expressed in terms of the average plasma parameters.

It is noted about the ordering employed in the neoclassical transport theory,

$$\rho/L <<< 1,$$

where L is the gradient scale length. The widely used common sense in the ambipolarity of the collisional transport (such that the like-particle collision does not contribute to the particle flux) relies on this assumption [30]. This assumption does not necessarily hold for the circumstances of the improved confinement. (A new name for the new ordering would be useful in clarifying the physics.)

3.1 Neoclassical Transport Coefficient

The plasma fluxes (particle, momentum, heat) have been expressed in terms of the gradients (density, velocity, temperature) and toroidal electric field. Since the toroidal electric field is in proportion to the electron-ion collision frequency, all the flux is in proportion to the collisional frequency. The result is summarized in literature [8,9] and details are not reproduced here. The flux is composed of two component; one for the axisymmetric plasma and the other due to the ripple trapped particles.

The influence of E_r on the axisymmetric component was found important if the parameter X defined as

$$X \equiv \rho_p E_r / T_i \, (= u_E) \tag{15}$$

becomes of order unity. For instance, the particle flux is affected as [31]

$$\Gamma^{NC} = -nD_p\left[\frac{n'}{n} + \gamma_j \frac{T'}{T} - \frac{e}{T}(E_r - B_\theta V_{||})\right]\exp(-X^2) \ . \tag{16}$$

In the plateau regime, $\gamma_j = 3/2$ and $D_p = (\sqrt{\pi}/2)(\varepsilon q \rho_i T/reB)$ for ions. The reduction comes from the shift of the transition region (between trapped-and-transit particles) to the higher energy region, in which less particle exists for Maxwellian plasmas.

The similar reduction is observed in the viscosity and could be important in the experiments [31,32]. There are three types of viscosity. Largest one is the bulk (or parallel) viscosity (denoted by μ_b). If the plasma moves in the direction of the magnetic field variation, the flow is resisted by the force $- m_i n_i \mu_b \nabla_{\|}^2 V_{\|}$. This force is of the order of $m_i n_i \nu_i \varepsilon^2 q^{-2} V_{\|}$ and is very large. In other words, the poloidal flow is damped by the time scale of the order of ν_i^{-1} in the absence of the radial electric field. The frictional force was given as

$$\langle B_\theta \cdot \nabla \cdot \vec{\Pi} \rangle = \frac{\sqrt{\pi}\varepsilon^2}{4r} m_i n_i v_{th} B (I_P V_\theta + I_T V_{p0}) \tag{17}$$

where V_θ is the poloidal velocity, $V_{p0} = -\rho_i v_{th,i} T_i'/2T_i$ is the drive due to the temperature gradient, and the numerical integrals I_P and I_T are given in [32]. The viscous force has a local maximum with respect to V_θ: Like a dynamic friction coefficient, it can be reduced at higher velocity. A useful formula, expressed in terms of the plasma dispersion function, is given in [33].

Other viscosity, i.e., the gyro-viscosity [34] and shear viscosity [35], are also subject to the influence of the radial electric field. It is noted in [35] that the collisional shear viscosity is less influenced by E_r, since mainly the transit particles contribute to this viscosity.

The influence of the radial electric field inhomogeneity could be also important. It was shown that the parallel viscosity can be expressed [36]

$$< B \cdot \nabla \cdot \vec{\Pi} > = \frac{1}{S^{3/2}} < B \cdot \nabla \cdot \vec{\Pi} >_0 \tag{18}$$

where Π is the stress tensor, and the suffix 0 denotes the expression in the absence of the inhomogeneous electric field. (For the explicit formula, see [36].) The influence on the flow and electric field is not simple as is shown in the next subsection.

The non-axisymmetric part (ripple diffusion) is more influenced. For instance, the particle flux associated with the helical-ripple trapped particles is given as

$$\Gamma_a^{NC} \simeq -\varepsilon^2 \varepsilon_h^{1/2} n \nu_D^2 \int_0^\infty dw \frac{w^{5/2} e^{-w} \nu(w)}{\nu^2 + 1.5\sqrt{\varepsilon/\varepsilon_h}\,\omega_{rot}^2} \left(\frac{n'}{n} - \frac{eE_r}{T} + \frac{(w - 3/2)T'}{T} \right) . \quad (19)$$

Similar result is calculated for the energy and momentum flux [9]. It is shown that when the resonance takes place,

$$\omega_{rot} \simeq 0,$$

the flux becomes large. If, on the contrary, E_r is very large, then the neoclassical flux is reduced in proportion to ω_{rot}^{-2}.

The formula (19) has advantage to give us an insight for the physics mechanisms. However, the deviation of particle orbit could be a system size for the ripple trapper particles, and the analytic formula may not be valid. The direct calculation based on the orbit computation in real geometry is sometimes used [37].

3.2 Loss Cone Loss (Direct Orbit Loss)

The influence on the loss cone boundary is important in the estimate of the loss cone loss. For the case of banana particles, the number density of particles in the ridge of the loss cone boundary is reduced. Thus the loss cone loss is estimated as

$$\Gamma^{lc} \approx n_i \nu_i \rho_p \exp\left(-X^2\right) \quad (20)$$

in the low collisionality limit [15]. It should be noted that the two aspects; (i) the like-particle collision (ion-ion in this case) causes the radial flux, and that (ii) the flux is not proportional to the gradient. More general formula was derived [32] in the collisionless limit as

$$\Gamma^{lc} \approx n_i \nu_i \rho_p \frac{\nu_*}{(\nu_* + X^4)^{1/2}} \exp\left[-(\nu_* + X^4)^{1/2}\right] \qquad (21)$$

where $\nu_* = \nu_i/\omega_b$ is the collision frequency normalized to the bounce-frequency.

3.3 Bootstrap Current

The Bootstrap current [38] has attracted special attention, because it is a typical example of the interference of various thermo-dynamical forces, and because it would be important in the fusion research in toroidal plasmas (such as the steady state sustainment of tokamak plasmas, or the possible current-driven instability in helical systems).

The effect of E_r on the axisymmetric part of the Bootstrap current (usual one for tokamaks) appears from the order of X^2. This is because the ions and electrons move together in the linear order of X. The Bootstrap current, and its counter part, Ware pinch [39], works primarily on trapped particles, and is the order of $\sqrt{\varepsilon}$. It is shown in Fig.4 that the number of trapped particles increases. The ion current, which is in the lower order in ε-expansion can appear if X becomes of the order unity.

The influence of the inhomogeneous radial electric field is subtle as well. As is shown in Eq.(18), the neoclassical viscosity tensor for ions are reduced (or enhanced) by the factor $S^{-3/2}$. This does not necessarily mean the enhancement (or reduction) of the plasma rotation and Bootstrap current. This is because the collisional friction forces are reduced by the same ordering: Owing to this proportionality, the ratios between them, which give the current and flow in steady state, do not explicitly include the

squeezing parameter S. The change of the effective collision frequency occurs, through which the result is affected [36].

The flux associated with the ripple trapped particle includes the linear correction with respect to the radial electric field. This is because the drift motion of electron and ions can be different if the collisionalities of electrons and ions are different. (Such a situation could happen that ions are in the 1/v-regime and electrons are not.) If so, the friction between them changes linearly to X. Although complicated it is, an explicit formula has been derived in [40]. Through the influence on the ion momentum balance, the Bootstrap current is also affected by the neutral particles [40].

3.4 Impurities

Collisional transport is important for impurities due to the higher ionic charge of such ions. Impurities have also heavier mass, so that the centrifugal force due to the radial electric field is more influential on impurity transport. In the banana regime it was given as [41]

$$v_{I,r} = \frac{m_i Z_I \nu_{ii}}{eB}\left[f_{trap}\frac{E_r}{B} + \frac{m_i}{reB}\left(\frac{E_r}{B}\right)^2\left\{\left(1+f_{trap}\right)\frac{A_I}{Z_I A_i} - 1\right\}\right] \qquad (22)$$

where the suffix I and i indicate impurities and main ions, respectively, Z is the charge and A is the mass number, and f_{trap} is the ratio of trapped particles ($f_{trap} \sim \sqrt{\varepsilon}$ holds in the absence of the strong magnetic field.) The first term in the right hand side is the inward pinch due to the collision with bulk ions, and the second term shows the centrifugal force. The centrifugal force can be outward [41,42]. Collisional transport theory predicts that the impurities are expelled from the plasma, if the radial electric field is strong enough

$$\frac{1}{v_{th}}\left|\frac{E_r}{B}\right| > \frac{r}{\rho_i}\frac{f_{trap}}{\left(1+f_{trap}\right)\frac{A_I}{Z_I A_i} - 1} \qquad (23)$$

This value seems too large to be realized except near the source of impurities, where A_I/Z_I is large.

4. Anomalous Transport

The anomalous transport has played more important role than the collisional transport, in the confinement of the hot plasmas. The influence of the radial electric field on the anomalous transport (and vice versa) is the important issue in understanding the plasma structure and dynamics in the confinement device. We discuss here the anomalous transport, among possible varieties, which is caused by plasma fluctuations.

The study on the anomalous transport has been developed by use of various methodology. The most well-established one is the quasi-linear theory, in which the characteristics of the microscopic perturbations are given by the linear response function of the plasma [43,44]. This method has lot of limitations in explaining the real plasmas, but could be instructive to understand the fluctuation and transport. Out of many work on this subject, some of the typical result is revisited here.

The nonlinear theory for the strong turbulence is, in the long run, inevitable to study the anomalous transport. The strong turbulence is characterized by the fact that the decorrelation rate of fluctuations is governed by the nonlinear interaction (through $\tilde{E}\times B$ Doppler shift in the electric turbulence) not by the linear growth rate. In this case, the inhomogeneous radial electric field is strongly influential. This problem will be next reviewed.

Based on these understanding, the recent theoretical pictures for the turbulent transport is discussed. As is well known, a lot of complicated transport phenomena has long been observed in plasmas (i.e., the radial-pressure-gradient-driven toroidal current or particle pinch associated with energy flow etc. [45]). These processes are

analyzed in the frame-work of the interference between thermodynamical fluxes and forces.

We here briefly discuss the ambipolarity of the turbulent driven flux, which is some times accepted *a priori*. If the turbulence is local, i.e., the waves emitted by electrons are absorbed by ions on the same magnetic surface, the momentum balance on each magnetic surface takes place: This leads to the ambipolarity. However, the fluctuations can often transmit momentum across the magnetic surfaces (e.g., the convective damping of drift waves [46]). Then the exchange of momentum between different magnetic surfaces takes place, and the shear viscosity appears. This contribution gives rise to the non-ambipolar (bipolar) component in the anomalous transport. It is in proportion to the curvature of the envelope of fluctuations [47]. Near the plasma edge, the convection can be more important. In the presence of strong inhomogeneity or near the edge, (i.e., the situation relevant to H-mode), the anomalous transport could play important role for electric field generation, which is discussed later.

4.1 Quasi-Linear Theory

4.1.1 Formalism

There are many instabilities in the plasma. The presence of the instability (frequency ω and wave number k) means that the (electro-magnetic) perturbation of the form $\exp\left(i\vec{k}\cdot\vec{x} - i\omega t\right)$ is emitted by plasma particles. In emitting the wave with the relevant momentum, the plasmas receive the force and drift in the radial direction. The method for the calculation is established, and, as in the case of the collisional transport, the relation between gradients (density, momentum, temperature) and the fluxes are derived. Explicit formula is given in literature [48]. For instance, the ion flux is given as

$$\begin{pmatrix} \Gamma_i \\ P_{\zeta r}/m_i v_{thi} \\ q_i/T_i \end{pmatrix} = \vec{\vec{M}}_i \begin{pmatrix} -\frac{n_i'}{n_i} + \frac{eE_r}{T_i} + \frac{T_i'}{T_i} - \frac{eB\omega}{k_\theta T_i} \\ -\frac{2V_\zeta'}{v_{th}} \\ -\frac{T_i'}{T_i} \end{pmatrix} \qquad (24)$$

where $P_{\zeta r}$ is the radial flux of the toroidal momentum, and q_i is the radial ion heat flux. The matrix element has the form like

$$M_{ij} = \frac{n}{B^2}\sum_k \int \frac{d\omega}{2\pi}\left(\frac{\omega}{\bar{\bar{k}}_{\parallel} v_{th}}\right)^{i+j-2} \frac{<\tilde{E}_\theta(k,\omega)\tilde{E}_\theta(k,-\omega)>}{|\bar{\bar{k}}_{\parallel} v_{th}|} \operatorname{Im} Z\left(\frac{\omega}{\bar{\bar{k}}_{\parallel} v_{th}}\right) \Lambda_0(b) \qquad (25)$$

being the second order term of the fluctuating electric field. In Eq.(25), $\Lambda_0(b)$ denotes the finite-gyroradius effect ($b = k_\perp^2 \rho_i^2$), and $\bar{\bar{k}}_{\parallel}$ is the effective parallel mode number, which ions feel in the presence of the radial electric field,

$$\bar{\bar{k}}_{\parallel}^2 = k_{\parallel}^2 + (k_\theta \rho_i)^2 (L_{n2} e E_r' T_i^{-1})^2,$$

$n'' = -nL_{n2}^2$. (Discussion on this effective $k_{\parallel}$ is given in [3,49].) Equation (24) shows the mobility term (i.e., E_r term in the right column), suggesting that it would be important for the interference of the transport. It is noted that the non-uniform part of the $E \times B$ rotation contributes to the mobility. The uniform part also appears in the Doppler shift of the wave frequency ω, and cancels each other.

In Eq. (24), however, the fluctuation amplitude is left undetermined. The contribution of the resonant particle, which appear in Eq.(25) does also appear in the expression of the linear growth rate, γ_L. The often-employed approximation, mixing length estimate, is that the fluctuation level is given by the ratio of the wave length to the gradient scale length,

$$\tilde{n}/n \sim 1/kL_n$$

(or $\tilde{E}_\perp \sim T/eL_n$). By the help of this approximation, an estimate

$$D \sim \frac{\gamma_L}{k_\perp^2} \tag{26}$$

is given [43]. This result is based on the picture that the nonlinear damping rate, $Dk_\perp^2$, balance with the linear growth rate. If one employs this formalism, the study of the effect of the radial electric field is reduced to the problem to analyze its effect on the linear stability.

4.1.2 Linear Stability

Two cases of the linear stability, i.e., the fluid like response and the Landau resonance, are shown here as typical examples.

The flute mode is a typical example of the plasma instability. In the presence of the pressure gradient ∇p parallel to the 'gravity' G (either real gravity or the centrifugal force due to the magnetic curvature) fluid-like instability can happen with $\gamma_L \sim \sqrt{G/L_p}$ ($L_p = -n/n'$ for $\nabla T = 0$). If the radial electric field exists, the plasma moves with the $E \times B$ velocity V_E in the direction perpendicular to the gradient. When the E-field is inhomogeneous, the perturbation (which is in the direction of g) is twisted in the direction of the $E \times B$ velocity V_E. As a result of this, the growth rate is deformed as [50]

$$\gamma_L = \sqrt{\frac{G}{L_p} - \left\{\frac{V_E'}{2kL_p}\right\}^2} \quad . \tag{27}$$

The off-resonant type stabilization is possible if

$$\left|V_E'/2kL_p\right| = \gamma_{L0} \quad . \tag{28}$$

γ_{L0} is the linear growth rate in the limit of $V_E' = 0$. This order estimate is applicable for the *linear stability* in the wide range, and is often employed in recent study on improved confinement [51]. This relation has similarity to the well-known stabilization by the diamagnetic drift,

$$\gamma_L = \sqrt{\gamma_{L0}^2 - \omega_*^2/4} \qquad (27')$$

where ω_* is the drift frequency, and γ_{L0} is the linear growth rate in the limit of $\omega_* = 0$.

Other type of the stabilization mechanism is seen in the wave-particle resonance. The Landau-damping is one of the main mechanism for the linear instabilities, and can also be important in the nonlinear mechanism. The ion motion is subject to the influence of the inhomogeneous radial electric field. It was demonstrated that the ion Landau damping, and associated stability for kinetic modes, are expected to occur for $\bar{\bar{k}}_{\parallel} v_{thi} \simeq \omega$ [3,49], or

$$\frac{L_{n2}\rho_i e E_r'}{T_i} \simeq \frac{\omega}{k_\theta v_{thi}} \ . \qquad (29)$$

Equation (13) also serves as a criterion that trapped ion mode disappears. Based on this mechanism, the reduction of the thermal transport coefficient in the H-mode was discussed [52].

4.2 Suppression of Turbulence

The formula (27) gives a first-step estimate, and Eqs.(28) and (29) provide a rough idea for the effect of the radial electric field inhomogeneity. The theory of the turbulence is necessary for the understanding of the turbulent-driven transport. The turbulence level is suppressed by E_r', and is discussed in this subsection.

Figure 6 illustrates the sheared flow and stretching the fluid element. The mean velocity is written as

$$V_y = S_v x$$

in the local coordinates. Consider the deformation of an element which is circular at t=0. The relative shift of the top to the bottom of the element is written as $LS_v t$ after the elapse of time of t, where L is the vertical size of the element. A circular element is stretched like an ellipse, the longer axis has the length

$$L_l \approx \sqrt{L^2 + (LS_v t)^2} \quad .$$

Since the area is preserved by this stretching, the length of the shorter axis is given as

$$L_\perp = \frac{L}{\sqrt{1 + S_v^2 t^2}} \quad . \tag{30}$$

This result shows that the perpendicular wave length is compressed. The deformation of the element is noticeable if it is of the order of L, i.e., $t \sim 1/S_v$.

4.2.1 Decorrelation and Damping due to the Shear Flow

These general considerations also apply to plasma turbulence. The flow velocity shear is interpreted as

$$S_v = r\, d(E_r B^{-1} r^{-1})/dr \; .$$

Noting the reciprocal relation between length L and wave-number $k_\perp$, the influence is calculated. The stretching of the turbulent vortex, Eq.(30), indicates that the perpendicular wave number is effectively enhanced by the factor [53-55]

$$k_{\perp eff}^2 = k_\perp^2 (1 + S_v^2 t^2) \ . \qquad (31)$$

After the consideration of Kadomtsev, the decorrelation rate,

$$1/\tau_{cor} \approx D k_{\perp eff}^2 \ ,$$

becomes larger by this increment of the perpendicular wave number. The elapse time t is limited by the decorrelation time τ_{cor}. Substituting the relation $t = \tau_{cor}$ in Eq.(31), the decorrelation rate $1/\tau_{cor}$ is given as

$$\frac{1}{\tau_{cor}} = D k_\perp^2 (1 + S_v^2 \tau_{cor}^2) \ . \qquad (32)$$

Two limiting cases are derived from Eq.(32) as

$$\frac{1}{\tau_{cor}} = \begin{cases} D k_\perp^2 + S_v^2 D^{-1} k_\perp^{-2} & (|S_v| << D k_\perp^2) \\ (D k_\perp^2)^{1/3} S_v^{2/3} & (|S_v| >> D k_\perp^2) \end{cases} \qquad (34)$$

This result shows that the decorrelation by the shear flow is more effective for the longer wave length mode. The limiting form of $\tau_{cor} \sim (D k_\perp^2)^{-1/3} S_v^{-2/3}$ is similar to the one which was derived by renormalizing the turbulent electron parallel motion in the sheared magnetic field [56].

The increased wave number suggests the reduction of the turbulence level. If one employs the ansatz of the mixing length estimate, $\tilde{n}/n \sim 1/k_{eff} L_n$, the level of fluctuation is reduced by the factor $k_\perp / k_{\perp eff}$ as

$$\frac{\langle \tilde{n}^2 \rangle}{\langle \tilde{n}^2 \rangle_{ref}} \approx \frac{1}{1 + S_v^2 \tau_{cor}^2} \qquad (34)$$

where the suffix ref indicates the reference case where $S_v = 0$ [53]. Using the large shear limit, $\tau_{cor} \sim (Dk_\perp^2)^{-1/3} S_v^{-2/3}$, the reduced fluctuations was discussed [54]. If one employs the Kadomtsev picture, the similar reduction factor is expected for the diffusivity.

These argument on the fluctuation level and transport, however, should not be taken as a conclusion. As was carefully discussed in [53], these analyses have been developed assuming that the basis of the fluctuations (such as the wave number $k_\perp$ of the relevant mode and so on) is unchanged. This term can also be a function of E_r and dE_r/dr. The effect of E_r and dE_r/dr, as a whole, can be determined after the turbulence is properly solved. (Numerical simulations have also revealed the subtle balance between various nonlinear interactions [57,58].) This problem is discussed in the section 4.3.

4.2.2 Statistical Property near Thermal Equilibrium

The decorrelation by the sheared flow has been subject to the intensive study in the fluid dynamics, which is instructive for the understanding. In the fluid dynamics or the phase transition physics, suppression of the fluctuations by the shear flow has been discussed. Before reviewing the turbulence in non-equilibrium plasmas, the study near the thermal equilibrium is revisited. The structure factor (form factor) of fluctuations

$$S(k) = \int d\vec{r} \exp(i\vec{k}\cdot\vec{r}) < \delta u(\vec{r} + \vec{r}_0)\delta u(\vec{r}_0) >$$

(δu being the fluctuating quantity) was calculated near the thermal equilibrium. Analytic expression was given [59]

$$S(\vec{k}) \simeq \frac{1}{\tau + k^2 + C|S_v k_y / L_k|^{2/5}} \qquad (35)$$

where L_k is the typical value for the kinetic (Onsager) coefficient, and is a coefficient denoting the damping in the Langevin equation. The inhomogeneous flow would efficiently suppress the fluctuations of the longer wave length. The structure factor is illustrated in Fig.7.

The size dependence is the characteristic feature of the shearing suppression. The case of the bubble formation was analyzed in [60]. If the shearing force $\bar{\mu}S_v$ is greater than the pressure change by the surface tension, $\bar{\sigma}/L$, the bubble is destroyed ($\bar{\mu}$ being the coefficient of fluid viscosity). The critical size $L_{cr} = \bar{\sigma}/\bar{\eta}S_v$, above which the bubble is destroyed, was found. On the other hand, there is a critical (minimum) size for the nucleation, L_{min} [61]. (This latter size is determined by the balance between the surface tension and the difference of the free energy within the bubble and fluid). If the velocity shear is strong enough so that the condition $L_{cr} < L_{min}$ (i.e., $S_v > \bar{\sigma}/\bar{\eta}L_{min}$) is satisfied, then the nucleation of the bubble is suppressed strongly.

4.3 Transport Matrix in Turbulent Transport

In this subsection, the study on the nonlinear turbulence is discussed. As is illustrated in Eq.(24) and in the case of neoclassical transport, the interferences between various thermodynamical forces and fluxes occur in the magnetized plasma. The relation between gradients and fluxes may be written as a matrix form. However, the expression in the matrix form is not validated *a priori*. The form like Eq.(24) suggests that the 'linear' relation between the gradient and flux. On the contrary, as we will see, the elements of the matrix strongly depend on the gradient. For instance, the factor like Eq.(34), which is also expected to appear in the transport coefficient, includes the inhomogeneity. The flux is given as a nonlinear function of various gradients; the efforts to separate one element as a 'gradient' and to leave the others in 'matrix element' retain some arbitrariness. Keeping this fact in mind, the 'diagonal' transport coefficient and 'off-diagonal' terms are distinguished here in a heuristic manner.

4.3.1 'Diagonal' Elements

The 'diagonal' transport coefficients are the basis for understanding the transport phenomena, and are discussed first.

In studying the influence of the electric field on the turbulent transport, one simplified method is a direct extension of the Kadomtsev formula. Keeping in mind the increment of the effective perpendicular wave number, Eq.(31), the mode growth rate is given as

$$\gamma_{NL} = \gamma_L - \frac{1}{\tau_{cor}} = \gamma_L - Dk_\perp^2(1 + S_v^2\tau_{cor}^2) \ . \tag{36}$$

In the stationary state, $\gamma_{NL} = 0$, or $1/\tau_{cor} = \gamma_L$, one has

$$D = \frac{\gamma_L}{k_\perp^2} \frac{1}{(1 + S_v^2\gamma_L^{-2})} \ . \tag{37}$$

This expression includes the effect of the radial electric field in two ways. First, the linear growth rate can be reduced as is discussed in Section 4.1. Second, the reduction of the mixing length by the shear flow gives a reduction factor.

The result is simple, and many linear stability analyses could be substituted into it. However, the relevance of the result is not clear, as was the case of Eq.(26). Test of the formula based on Eq.(26) has been performed with exhaustive review on various unstable mode (see e.g., [44,62]). The result was, however, far from satisfactory. Because the form (26) seems to be incomplete, the extensions, Eq.(37), would be limited in applicability to real plasmas.

The transport coefficient could be different from the form like Eq.(26), if the mode growth is affected by the nonlinear interactions. This is really the case. The analysis on the electron nonlinearlity has shown that the drift wave in a sheared slab (which is known to be linearly stable [63]) can be unstable if the fluctuation amplitude

is large enough [56]. Examples of nonlinear instability have been found through numerical simulations for drift waves [64].

The stationary state is realized by the condition, noting the *nonlinear growth*,

$$0 = \gamma_{NL} = \gamma_{ng} - \frac{1}{\tau_{cor}} \tag{38}$$

in which the suffix ng indicates the growth by the nonlinear process. The nonlinear instability was shown to dominate over the linear one by the electron nonlinearlity [65]. The balance, $\gamma_{ng} \approx 1/\tau_{cor}$, indicates the fact that both the growth and damping are caused by nonlinear interaction. In other words, the steady state turbulence is self-sustained. A comparison of this picture with that of Kadomtsev formula is given in Fig.8.

The self-sustained turbulence is solved in analytic manner for ballooning mode turbulence and interchange mode turbulence. By renormalizing the nonlinearlity associated with the Lagrangean derivative, $\tilde{\nabla}\nabla$, the equation for the test mode is obtained, which includes nonlinear interactions in terms of the diffusion operator. For the simplicity, the one for the interchange mode turbulence is shown as [66]

$$\begin{aligned} &\frac{d}{dk}\frac{k_\perp^2}{\gamma + \lambda k_\perp^4}\frac{d}{dk}\left(\gamma + \chi k_\perp^2 + \omega_{E1}\frac{d}{dk}\right)\tilde{p} + \frac{G_0}{s^2}\tilde{p} \\ &- \frac{1}{k_\theta^2 s^2}\left(\gamma + \mu k_\perp^2 + \omega_{E1}\frac{d}{dk}\right)k_\perp^2\left(\gamma + \chi k_\perp^2 + \omega_{E1}\frac{d}{dk}\right)\tilde{p} = 0 \end{aligned} \tag{39}$$

where G_0 is a combination of the pressure gradient and bad curvature, $G_0 = \Omega'\beta'/2\varepsilon^2$, s is the magnetic shear parameter, and (μ, λ, χ) are the *renormalized* viscosity, current diffusivity and thermal conductivity, respectively.

$$\omega_{E1} = k_\theta E_r'/Bv_{Ap}$$

denotes the shear flow velocity due to the inhomogeneous radial electric field (v_{Ap} is the poloidal Alfven velocity). If one neglects the renormalized transport coefficient, it describes the linear interchange instability. The stationary state is obtained to give

$$\chi \sim \frac{1}{(1+0.5G_0^{-1}\omega_{E1}^2)} \frac{G_0^{3/2}}{s^2} \left(\frac{c}{\omega_p}\right)^2 \frac{v_{Ap}}{a} \tag{40}$$

with the ion and electron viscosities of the same magnitude [66]. The typical correlation length of the fluctuations is dependent on the pressure gradient,

$$\langle k_\perp^2 \rangle \propto (1+0.5G_0^{-1}\omega_{E1}^2)/G_0 \ . \tag{41}$$

The saturation level

$$\frac{e\tilde{\phi}}{T} \sim \frac{1}{(1+0.5G_0^{-1}\omega_{E1}^2)} \frac{G_0^{3/2}}{s^2} \left(\frac{c}{\omega_p}\right)^2 \frac{v_{Ap}}{a} \frac{eB}{T} \tag{42}$$

is obtained simultaneously. Fluctuations are expressed in terms of the structural parameters. These results show that the correlation length becomes shorter and the fluctuation level decreases owing to the electric field shear. Compared to Eq.(31), we see that the correlation time is consistently determined in Eq.(41). What is important is that the correlation length becomes longer and fluctuation level gets higher as the pressure gradient increases. These features are the characteristics of the transport process in the non-equilibrium matter. (It is in contrast to the collisional diffusion, which is generated by the thermal fluctuations, i.e., Coulomb collision.)

The same argument is extended for the tokamak plasma transport based on the ballooning mode turbulence. The result is given as

$$\chi \sim \frac{1}{(1+h_1\omega_{E1}^2+h_2\omega_{E2}^2)} \frac{\alpha^{3/2}}{f(s,\alpha)} \left(\frac{c}{\omega_p}\right)^2 \frac{v_A}{qR} \tag{43}$$

where $\alpha = -q^2R\beta'$, and numerical coefficients (h_1, h_2, f) are functions of s and α (see [67] for the details.) ω_{E2} denotes the curvature of the radial electric field. The ion viscosity also follows the formula Eq.(43). The characteristic scale length of the fluctuations is also shown to decrease by a similar factors if the electric field shear is increased.

The result Eq.(43) (or Eq.(40)) indicates that the electric field inhomogeneity, as a whole, suppress the anomalous transport. The efficiency for the suppression (the coefficient to the inhomogeneity parameters) depends on the pressure gradient and other plasma parameters. Both the gradient and curvature of the electric field is effective in reducing the transport coefficient. The formula Eq.(40) and (43) show that the pressure gradient enhances the anomalous transport. This is the one of the main features of the anomalous transport in confined plasmas.

4.3.2 'Off-Diagonal' Elements

The phenomena like rotation drive by the pressure gradient or the Bootstrap current is analyzed by studying the off diagonal elements in the nonlinear transport theory. In the renormalization of the Lagrangean derivative, the matrix formula is obtained. For instance, the one point renormalization gives the torque, the driving force for the current and the heating as a function

$$-\nabla\cdot\vec{D}\begin{pmatrix}\nabla_r E_r' \\ \nabla_r J \\ \nabla_r p\end{pmatrix} \qquad (44)$$

where J is the parallel current, and the elements of the matrix D is given by fluctuations and decorrelation rates [65]. (Notice that the vorticity is proportional to E_r'.) We do not present a lengthy and explicit form of the matrix elements. Some processes, which is useful to derive a simple model dynamical equations later, will be reviewed here.

4.3.2.1 Generation and Damping of the Flow

It is well known that the inverse-cascade takes place in the plasma, and the microscopic fluctuations accumulates to give rise a global structure [68]. Anomalous transport can cause selective loss of ions or electrons, as well. The radial electric field and the associated poloidal flow, which are generated by plasma fluctuations, have been studied intensively in relation with the H-mode physics [15]. If one writes the equation for the poloidal motion in the absence of the radial current, it contains the terms

$$\frac{\partial}{\partial t}\overline{P_\theta} = -\frac{\partial}{\partial r}\overline{\langle \tilde{V}_r \tilde{P}_\theta \rangle} - \frac{2T}{R}\overline{\cos\theta \frac{\partial}{\partial \theta} n} \qquad (45)$$

where the over bar indicates the average on the magnetic surface.

The first term is understood as the convection of the momentum. If the perturbation of momentum $\tilde{P}_\theta$ is in phase of the radial velocity fluctuation $\tilde{V}_r$, there appears a net radial flux of the poloidal momentum. An example of the flow pattern in fluctuations, which has the correlation between $\tilde{P}_\theta$ and $\tilde{V}_r$, are shown in Fig.9. In this case, $\tilde{P}_\theta$ takes positive (negative) value if $\tilde{V}_r$ is positive (negative). The average $\langle \tilde{P}_\theta \tilde{V}_r \rangle$ does not cancel out, but gives finite values. The divergence of this flux appear as a local force.

Important is the task to evaluate the phase relation between $\tilde{P}_\theta$ and $\tilde{V}_r$, as the phase relation between $\tilde{n}$ and $\tilde{V}_r$ is an important issue in determining the particle flux. This term has been discussed by physical considerations. Some example is shown in [69,70]. This term is quadratic in fluctuations and is proportional to $k_\theta k_r^2$ because of the three derivatives involved. There is no preferential momentum in the absence of the symmetry braking; therefore it is proportional to $k_\theta V_E'/k_r\gamma_0$, ($\gamma_0$ being a scale of the growth rate of the mode). Based on these dimensional considerations, one has an analytic estimate for the turbulent driven torque as

$$\frac{\partial^2}{\partial r^2}\overline{\langle \tilde{V}_r \tilde{P}_\theta \rangle} \simeq -\frac{k_\theta^2 k_r^2 n v_{thi}^2 \rho_i^2}{\gamma_0} \left|\frac{\tilde{n}}{n}\right|^2 V_E' \quad . \tag{46}$$

Assuming that the mode characteristics (k and γ_0) are given by those for the linear waves, explicit expressions for various instabilities were given in [69]. Although the validity of the linear counterpart is not clear, the dimensional dependence like Eq.(46) may have a wide applicability if the mode characteristics are properly chosen. This kind of study is widely developed in literature [71].

The second term is the toroidal correction [72]. An up-down difference of the pressure is expected in the toroidal plasma and can give rise to a rotation [73]. The influence of the gyro-viscosity appears through the up-down asymmetry [34]. Such a term could also be important for the anomalous transport, if it has also poloidal inhomogeneity. An expression was derived

$$\frac{2T}{R}\overline{\cos\theta \frac{\partial}{\partial\theta} n} \simeq \frac{q^2}{\varepsilon}\frac{1}{n}\overline{\cos\theta \frac{\partial}{\partial r}\langle \tilde{V}_r \tilde{n} \rangle}\,\overline{P_\theta} \quad . \tag{47}$$

This term is also proportional to the average poloidal momentum. If there is no poloidal rotation in the beginning, there is no asymmetry in the plus θ and minus θ direction. In such a case, the $\cos\theta$ component of the radial flow does not make the poloidal rotation.

Both the terms Eq.(46) and (47) are in proportion to the original global flow. The mechanism in Eq.(45) enhances the global flow and its structure, if there is a seed of the global flow. This feature resembles to the situation of the dynamo problem. For instance, the α- and β- dynamos are proportional to the average magnetic field and to the current, respectively. A seed component of the global scale is required. Also the common physics to the solar dynamics [74] was pointed out . The generation of the flow by the fluctuations is expected when the mirror-symmetry does not hold. The density gradient can also generate the poloidal flow and radial electric field. It was shown that the potential energy have nature of inverse cascade, if the parallel electron

motion is impeded [57]. Numerical simulation has shown that as the fluctuations develop, the zonal flow is generated [57,58,72,75].

The estimate for the anomalous torque must be developed using the same theory that is used in analyzing the diagonal terms. Hopefully, it could explain the experiments on the diagonal elements in the transport flux. Theory of the self-sustained turbulence was extended to estimate Eq.(44) as [76]

$$P_{\perp r} = -m_i n_i \mu_\perp \left\{ \nabla V_E + \frac{M_{12}}{M_{11}} v_{Ap} \nabla^2 \beta \right\} \tag{48}$$

with $\mu_\perp = \chi$ and $\frac{M_{12}}{M_{11}} \simeq \frac{f^2(\alpha,s)}{4\varepsilon} \sqrt{\frac{m_i}{m_e}} \frac{c}{\omega_p}$.

4.3.2.2 Anomalous Bootstrap Current and Dynamo

Anomalous Bootstrap current is known to be small in toroidal plasmas. This is because the wave vectors of fluctuations are mainly in the poloidal direction, and not much momentum in the parallel direction is exchanged by electrons [48,77]. The importance of the dynamo term is also pointed out in relation to the structural formation in the L-H transition [78]. The interference of the current generation and flow generation was discussed. The mechanism is found to be effective in the large scale dynamics (like celestial plasma) and its application to the laboratory plasma remains for future problem [79].

5. Structural Formation and Improved Confinement

In this section, we study the mutual interaction between the radial electric field and the plasma profile. First, the mechanism of the radial electric field generation is discussed. Each element, which contributes to the E-field generation, could be dependent on the radial electric field or its derivative. Thus the self-consistent picture for the structural formation of the radial electric field and plasma is obtained. Several

approaches to derive a set of closed equations with simplified variables are shown. Finally, the theoretical predictions from theories are discussed.

5.1 Contraction of Variables

The number of variables which describes the plasma state is huge. It is therefore an important task to choose the essential variables and reduce the complexity of the equations. In the plasma, there are lots of potentially-unstable eigenmode of perturbations. The theory which includes a complete set of variables should not be, undoubtedly, solvable nor increasing our understanding. At the same time, the variables should not be limited to those observed in experiments. The understanding of the transition phenomena could become possible by introducing the 'hidden variable', the radial electric field [15].

The reduction of the variable is essential, as has been in the case of non-equilibrium statistical physics, the physics of chemical reaction, the diffusion-reaction problems or the fluid dynamics. Historically, there have been many useful model equations, e.g., Ginzburg-Landau equation, Langevin equation, Lorenz model, Brussellator, Oregonator, etc. [80]. In the following, the contraction of the variable will be introduced from two processes. In one approach, variables to be contracted change rapidly, so that they are approximated to be in a stationary state and controlled by the other variables; The dynamics of the latter variables are analyzed, and the value of the rapidly-changing variable is evaluated by the equilibrium equation. The other is the statistical average. One or few moments are chosen as variable, and the other internal freedom is neglected. Even within this primitive state of the theoretical progress, some of the varieties in the plasma can be illuminated and explained.

5.2 Generation of Radial Electric Field

The radial electric field is generated by the radial current. If ions go out faster than electrons, then the radial electric field becomes more negative. The Poisson's equation can be written as

$$\varepsilon_0\varepsilon_\perp \frac{\partial}{\partial t} E_r = e(\Gamma_e - \Gamma_i) \tag{49}$$

where $\varepsilon_\perp$ is the perpendicular dielectric constant, Γ_e and Γ_i are the radial fluxes of electrons and ions, respectively.

The stationary state equation,

$$\Gamma_e[X, X'; \nabla p \cdots] = \Gamma_e[X, X'; \nabla p \cdots] \tag{50}$$

determines the structures of the radial electric field as a function of the plasma profiles, $X(r\,;\, \nabla p \cdots)$. The thermal transport coefficient is also a nonlinear function of the radial electric field structure, as is given by Eqs.(40), (43), and have a complicated form due to the generation of the radial electric field. It should also be noticed that Eq.(50) is the nonlocal equation to determine the structure. As has been seen in the previous sections, the particle loss such as the orbit loss, is not a local quantity, but is determined by the global information of the radial electric field in the plasma column. Equation (50) must be considered as an equation that determines the global structure simultaneously including the long-distance interaction.

Much has been analyzed on Eq.(50). The L-H transition physics is discussed in detail in the following section. In addition to the H-mode physics, examples of theoretical study include the radial electric field structure in the core of helical plasmas [4, 81]. For the plasma in helical systems, the electric field effect on the collisional transport could be as important as the anomalous transport. The collisional transport theory has shown that the formation of the negative radial electric field as well as the positive electric field, depending on the collisionality.

5.3 Bifurcation

Equation (50) predicts the bifurcation of the solution X (X' and X", as well). Since plasma transport coefficients are dependent on the electric field structure, this bifurcation in the radial electric field causes those in the plasma transport. The nature of the bifurcation is discussed as a main working hypothesis to understand the H-mode physics.

5.3.1 Hard and Soft Bifurcation

Theories on the H-mode are classified into two, depending on the relation between the gradient and flux. Figure 10 illustrates, for the two cases, the relation between the particle and heat fluxes, radial electric field and fluctuation level, as a function of the gradients ∇ n and ∇T. Figure 10(a) shows the *hard transition* model. In this case, the flux (and fluctuation level and so on) takes multiple values at certain values of the fixed gradients. Figure 10(b) presents those for the *soft-transition* model. In the latter model, the flux can be a decreasing function of the gradients, but is a single-value function. If the system has the nature of the hard transition, the soft transition is also available by the change of parameters. Summarizing the continual change, the cusp-type bifurcation (for the case of the hard transition) is obtained [24]. The change from the low confinement state to the high confinement state ("A" to "B" in Fig.10(c)) could occur either by crossing the transition points, or by following a smooth change as is illustrated.

The Itoh-Itoh model and Shaing model belong to the case of hard transition [15,32]. Those in [14, 69, 71, 82] belong to the class of soft transition. Instead of reproducing results in many theories, we will try to clarify the physics out of various models of transitions.

5.3.2 Hysteresis and Limit Cycle

The hard transition model can predict the fast transition at the critical points. This system has the hysteresis and can generate the limit cycle oscillation. Figure 11 illustrates the loss rate as a function of the plasma parameter in the case of the hard transition type [83]. This curve is seen as a family of the *backward* bifurcation (which usually appears in the sub-critical turbulence). There is a hysteresis as is shown by the dotted line. The central branch is thermodynamically unstable, so that the limit cycle oscillation is possible. Let us consider the situation that the critical condition is reached under the condition that the global parameter changes gradually. As is shown later, the limit cycle oscillation appears suddenly at the critical point. This dynamics is discussed later in relation to ELMs (Edge localized Modes [84]).

The hysteresis also exists in the case of soft bifurcation. This belongs to a class of normal bifurcation (pitch-fork bifurcation). The limit cycle oscillation can also be available in this type. Like Hopf bifurcation, the limit cycle appears gradually under the gradual change of the global parameter. This is one of the points that discriminates the relevance of the model.

The hard transition can in principle happen sequentially. In such a case, chaotic behaviour or intermittence of the bursts can appear. These problems has been studied intensively in statistical physics (e.g., [85]), but not much work has been done in plasma transport theory.

5.3.3 Mechanisms to Generate Bifurcation

As was discussed in previous sections, there are many processes which are associated with the radial current. If one writes the equation, for singly charged ions, in terms of the radial electric field, one has

$$\frac{\varepsilon_0 \varepsilon_\perp}{e} \frac{\partial}{\partial t} E_r = \Gamma_{e-i}^{anom} - \Gamma_i^{lc} - \Gamma_i^{bv} - \Gamma_i^{v\nabla v} - \Gamma_i^{NC} + \Gamma_e^{NC} - \Gamma_i^{cx} \qquad (51)$$

The terms in the right hand side represent the following processes. (i) Γ_{e-i}^{anom} is the contribution of the bipolar part of the anomalous cross field flux (i.e., the excess flux of electrons relative to that of ions), examples for which was discussed as Eqs.(46) and (48). (ii) Γ_i^{lc} is that from the loss cone loss of ions (Eq.(20) or (21)). (iii) Γ_i^{bv} is due to the bulk viscosity coupled to the magnetic field inhomogeneity. (iv) $\Gamma_i^{v\nabla v}$ is the Reynolds stress in the global flow, which includes the one due to the toroidicity like Eq.(47). (v) Γ_i^{NC} and Γ_e^{NC} are contribution of the collisional flux (e.g., the ripple diffusion, Eq.(19), or the contribution of the gyro-viscosity). (vi) Γ_i^{cx} is the ion loss owing to the charge exchange [24,53,86]. It should be noted that the external-driven rf-waves can contribute to the term of Γ_{e-i}^{anom} [87]

Each of these terms has a dependence on the radial electric field, as is shown in previous sections. In order to have a perspective, we choose some of the characteristic terms. Qualitative dependencies of these terms are shown as

$$\Gamma_{e-i}^{anom} \sim \hat{D}[X,X'](\lambda_p - X) + \hat{\mu}_\perp[X,X']\hat{\nabla}_\perp^2 X \tag{52-1}$$

$$\Gamma_i^{lc} \sim f_{lc}\nu_i\rho_p n_i \exp(-X^2) \tag{52-2}$$

$$\Gamma_i^{bv} = \frac{\varepsilon^2 n_i T_i}{erB}(X + X_0)\,\mathrm{Im}\, Z(X + i\nu_{**}) \tag{52-3}$$

where $\lambda_p = -\rho_p(\nabla n/n + \alpha_0 \nabla T/T)$ is the normalized gradient [15], $Z(X + i\nu_{**})$ is the plasma dispersion function [88], $X_0 = -\rho_p(n'/n + \gamma_{NC}T_i'/T_i) + V_{i\parallel}/v_{thi}$, and $\nu_{**} = \nu_i qR/v_{thi}$. Numerical coefficient f_{lc} is a function of the geometrical factor such as ε. The formula (52-3), which is useful for both the banana and plateau regime is given in [33]. In the more collisional case, Eq.(52-3) has the limiting form as

$$\Gamma_i^{bv} \sim \varepsilon^2\nu_i\rho_p n_i \frac{X + X_0}{\nu_{**}^2 + X^2} \quad . \tag{52-3'}$$

The form of the radial flux due to the charge exchange with neutral particles are given as

$$\Gamma_i^{cx} = -n_0 \langle \sigma_{cx} v \rangle n_i \rho_p \left(X_0 + X - qV_p/\varepsilon v_{th} \right) \qquad (52\text{-}4)$$

where n_0 indicates the density of the neutral particles and $\langle \sigma_{cx} v \rangle$ is the charge exchange cross section. In the case that the plasma is rotating in the toroidal direction, Eq.(52-4) reduces to the form of friction in proportion to $(X_0 + X)$.

Bifurcation of the hard transition type has been found by combining Eqs.(50) and (52). The first example is the analysis on the balance between Γ_{e-i}^{anom} and Γ_i^{ic} [15] and the other is that between Γ_i^{ic} and Γ_i^{bv} [32]. Figure 12 illustrates these examples of the bifurcation. It is seen from this figure that the radial electric field shows the hard transition at critical plasma parameters. The bipolar part of the plasma flux, shown by Eqs.(51), (52) jumps at the critical point as well.

5.3.4 Dielectric Constant and Time Constant

The dielectric constant $\varepsilon_\perp$ determines how fast the stationary state Eq.(50) is realized. In the magnetized plasma, the dielectric constant takes a large value. This is because the polarization drift of ion screens the charge separation of the flux. As the radial electric field starts to increase, so does the cross-field $E \times B$ velocity. The acceleration in the cross-field velocity causes the radial drift of ions. This ion drift is in the direction to reduce the change of radial electric field. In the slab plasma, it was given as

$$\varepsilon_\perp = 1 + c^2 v_A^{-2} \approx c^2 v_A^{-2} \ . \qquad (53)$$

In toroidal plasmas, this coefficient can be enhanced [78]. As is discussed in relation to the Pfirsch-Shluter current or to the damping of the poloidal flow, the flow

in the poloidal direction can be coupled to the toroidal flow, since the plasma flow is nearly incompressible, $\nabla \cdot V \approx 0$ [2]. If the flow is constrained on the magnetic surface, as is treated in the neoclassical theory, i.e., $V_r = 0$, the divergence of the poloidal flow $\nabla_\perp \cdot V_p$ must be compensated by the parallel divergence $\nabla_\parallel \cdot V_\parallel$. The poloidal flow V_p leads the parallel flow like $V_\parallel \sim (2q \cos\theta) V_p$. (See Fig.13(a)). If this enhancement is taken, the dielectric constant is multiplied by the enhancement factor M_{eff}, as

$$\varepsilon_\perp^{tor} = M_{eff} \varepsilon_\perp \tag{54-1}$$

$$M_{eff} \simeq 1 + 2q^2 \tag{54-2}$$

(more generally, M_{eff} also depends on the collisionality and X. See, e.g., [89-91] for the details in the neoclassical theory.)

This neoclassical enhancement may not appear in the L-H transition, because the plasma flow is not necessarily limited on the magnetic surface (Fig.13(b)). The divergence of the poloidal flow can be compensated in a different way, namely, $\partial V_r/\partial r \approx -r^{-1} \partial V_\theta/\partial\theta$. In a thin layer (width ℓ) near the edge, the radial velocity of the order

$$V_r \sim (\ell/R) V_\theta \sin\theta \tag{55}$$

is enough to balance the divergence of the poloidal flow. This sine-dependence of the radial flow is generated by the poloidal inhomogeneity of the static potential. As is discussed in section 5.4.3, much larger radial flow with $\sin\theta$ dependence could be possible. The analysis of the dielectric constant in toroidal plasma with inhomogeneous radial flow remains future analysis.

5.4 Spatial Structure and Dynamics

The two characteristic features of the H-mode, i.e., the steep gradient formation and the rapid transition, can be analyzed by considering the spatial-temporal dynamics based on the evolution equation. The space-time dynamics based on the bifurcation equation is discussed in this section. Along the method of contraction of variables, we first survey the types of the model equations. Then the prediction out of the model formula is reviewed.

5.4.1 Model Equations

The system of equations includes the nonlinearlity, bifurcation and spatial diffusion and dissipation. In order to fully understand the dynamics of the problem, the nonlinear diffusion equation with the bifurcation is necessary. This type of the model is first studied. Then the point model is visited. By properly choosing the scale length, the local model (point model) would tell fruitful physics out of the simple and tractable equations. For instance, the Lorenz model is one of the most famous model equation of this kind.

5.4.1.1 Extended Ginzburg-Landau Type Equations

The transport equations of the plasma parameters and the electric field are given in a symbolic form by using the nonlinear transport coefficients (e.g., Eqs.(40), (43), (51) and others) as

$$\frac{\partial}{\partial t}n(r) = \nabla \cdot D[X, X'; n(r), T(r), \cdots] \nabla n(r) + S_p \qquad (56\text{-}1)$$

$$\frac{\partial}{\partial t}T(r) = \nabla \cdot \chi[X, X'; n(r), T(r), \cdots] \nabla T(r) + P \qquad (56\text{-}2)$$

$$\upsilon\frac{\partial}{\partial t}X(r) = \nabla \cdot \mu[X, X'; n(r), T(r), \cdots] \nabla X(r) + N[X, X'; n(r), T(r), \cdots] \qquad (56\text{-}3)$$

where S_p is the particle source and P is the heating power. The coefficient υ indicates the fact that the time scale in Eq.(51), determined by the flux and viscosity, may be much faster than the usual transport process for the temperature and density. The nonlinear term N in Eq.(56-3) indicates those source terms of the radial electric field in Eq.(51), which allow the bifurcation of the hard transition type. The choice of the transport coefficient like

$$\mu = \mu[X, X'; n(r), T(r), \cdots] \tag{57}$$

represents the stand point of variable contraction; In other words, the characteristic time for the change of the turbulence is much faster than that of the plasma parameters. As plasma parameters and profiles change, the fluctuation develops so fast that the stationary relation Eq.(57) is immediately established. This approximation is based on the assumption of the time scale separation. These forms of the set of equations belongs to the type of the extended-time-dependent Ginzburg-Landau equation (E-TDGL equation), and has been used in [83,92,93]. (The term of 'extended' indicates that the set of equations (56) includes the diffusion terms.)

5.4.1.2 Zero-Dimensional Model

The system of equations (56) includes the information of the time and space simultaneously. By replacing the operator ∇ with numbers, the set of equations reduces to the one for a local variables by straightforward rewriting. The E-TDGL type equation was reduced to the one-point model in [92], and similar result with those from Eq.(56), including the hard transition, was confirmed. With these expression of the terms in Eq.(51), and Eq.(53), the radial electric field changes in the time scale of the order of

$$\tau_{tr} \sim (\varepsilon/q)^2 \nu_i^{-1}$$

[24]. If one employs the neoclassical dielectric constant, it becomes longer as by the factor, q^2, $\tau_{tr} \sim \varepsilon^2 \nu_i^{-1}$.

Other type of the bifurcation (e.g., soft-type) is also modelled in a local dynamical model. An example is given, e.g., in a form of the set equations for the plasma pressure, the electric field inhomogeneity and the fluctuation level as [69]

$$\dot{A} = \gamma_0 A - \alpha_1 A^2 - \alpha_2 UA \tag{58-1}$$

$$\dot{U} = -\mu U + \alpha_3 AU \tag{58-2}$$

$$\dot{G} = -\alpha_5 G - \alpha_4 GE + P \tag{58-3}$$

where A denotes the fluctuation level, $A \sim |\tilde{n}/n|^2$, U the flow shear, $U \sim |V_E'|^2$, G the pressure gradient, and P denotes the heating power, respectively. (Expression of the coefficients α_j in terms of the linear mode characteristics are given in [69].) This particular form was derived by the dimensional argument, and is not necessarily unique. Similar, but not identical, zero-dimensional dynamical models are given by other groups (say, [71]). The set of Equations (58) is shown here just as a representative one in this kind. This type of the dynamical model has two types of the steady states, i.e.,

$$(A = \gamma_0/\alpha_1,\ U = 0),$$

$$(A = \mu/\alpha_3,\ U = (\gamma_0 - \alpha_1\mu/\alpha_3)/\alpha_2).$$

These two branches merge smoothly at the condition $\gamma_0\alpha_3 = \mu\alpha_1$. The soft transition (Hopf bifurcation) is predicted. These type of the models would be useful in analyzing the phenomena of the soft transition.

5.4.2 *Interface of Domains*

The spatial structure has a vital importance, because the inhomogeneity of the radial electric field is one of the important mechanism for the reduced transport. Based on the set of equations (56), the spatial structure has been solved. An analytic insight is discussed here and the detailed transport simulation is discussed later.

As is shown in Eq.(56), this problem is the investigation of the interface formation in the media which has multiple states (like the L- and H-phases in this case). For the clarity of the argument, a simplified model of Fig.11, which allows the bifurcation with hard transition, is employed [84,92,93]. As the plasma parameter changes in radius, the controlling parameter of the states (i.e., the abscissa of Fig.11) varies. As a result of the multiple solutions in a steady state equation (50), the possible solution of the radial electric field (and transport coefficients as well) distributes in space as is illustrated in Fig.14. At each plasma location, the electric field takes one value at one time; there should appear the interface, across which the different branch of the solution touches. The viscosity does not allow the change in an infinitesimal distance. The two branches are connected by the layer of finite width following the E-TDGL equations in Eq.(56). In this layer, the value of the radial electric field takes the value in between the high- and low-solutions. Therefore it is called as a *meso-phase*.

Work has been done to analyze the nature of the interface, in the motivation to study, first, the electric field in the non-axisymmetric systems [94,95] and the concept of the Ambi-polaron [94] was proposed. The interface layer was found to be thermodynamically stable in the neoclassical theory: This layer can drift in radial direction until it reaches the stationary state, and the stationary solution is proved to be unique for given plasma parameters. The dynamics requires, in other words, the processes discussed in section 5.3. Under the condition that plasma profile is constant in time and changes in space more gradually than the layer width, the location of the

interface was discussed [95,96]. The condition determines the parameter g (the parameter in Fig.11 controlling the electric field and transport) by the equation

$$\Delta\Phi(g) = 0 \tag{59-1}$$

$$\Delta\Phi(g) \equiv \int_{X_l}^{X_u} \{\Gamma_e[X; g] - \Gamma_i[X; g]\}\, dX \tag{59-2}$$

where X_u and X_l are the solution X[g] on the upper branch and lower branch, respectively, of Fig.11. This relation is counterpart of the *Maxwell's construction* (Maxwell's Rule of Equal Areas) at the phase transition in the thermodynamics [97].

5.4.3 Poloidal Structure and Shock Formation

The fast rotation associated with the radial electric field structure can change the poloidal structure in toroidal plasmas.

The influence of the centrifugal force associated with the toroidal rotation has been discussed in the framework of the neoclassical theory. Ions are abundant in the low field side of the torus due to the centrifugal force, and the potential can be higher in the low field side than in the high field side. The inhomogeneous part of the static potential has been calculated as[35]

$$\frac{e\tilde{\phi}_0}{T_e} = \frac{\varepsilon V_\zeta^2}{c_s^2}\cos\theta \tag{60}$$

where the suffix 0 indicates the stationary state. This gives the in-out asymmetry of the density and up-down asymmetry in the E× B velocity.

The fast poloidal rotation associated with the electric field bifurcation can cause the poloidal shock in tokamaks. Theoretical study has been first performed about the shock formation analyzing the fast flow of the order of the sound velocity [98].

Because the experimental plasmas at the 70s was far from the condition which is necessary for the shock formation (and so was the theoretical prediction of the neoclassical transport theory), the progress in the shock formation has waited the evolution of the H-mode physics [82,99].

The poloidal flow compresses itself as the fluid element moves from the outside of the torus to the inside. After [99], the equation is given in a form of the Burgers equation with the external force,

$$\frac{\partial}{\partial t}V_p + V_p\frac{\partial}{r\partial\theta}V_p - \frac{\mu}{2}\frac{\partial^2}{r^2\partial\theta^2}V_p = -\frac{F_p}{2}\sin\theta \qquad (61)$$

where F_p stands for the effective force due to the toroidicity, and μ is related to the bulk viscosity (rather than the shear viscosity). This is the limit that the terms Γ_i^{bv} and $\Gamma_i^{v\nabla v}$ of Eq.(51) is kept explicitly and the sine components of other terms are rewritten as the effective external force. The term of the dispersion ($\partial^3/\partial\theta^3$, the third derivative with respect to the poloidal angle) is small for the parameters of our interest, and is omitted here. Equation (61) describes the simple diffusion equation, if the force and the flow is small. As was explained in Eq.(51), large electric field and high poloidal velocity are possible if terms in the right hand side of Eq.(51) become significant.

As the torque for rotation, F_p in Eq.(61), becomes large, high plasma rotation (the poloidal Mach number, X, of the order unity) is possible. In such a situation, the poloidal distribution of the velocity and the density are not uniform. An example is shown in Fig.15. This implies the weak shock like formation in the poloidal direction. As a result of this, there appears the up-down asymmetry of the density and the poloidal flow. The static potential is not constant on the magnetic surface, and has a poloidal variation, of the order of

$$|\tilde{\phi}_0| \sim \sqrt{\varepsilon}T_e/e \ . \qquad (62)$$

The radial flow which has the parity of $\sin\theta$ appears. This value easily come to (or exceeds) the level of Eq.(55).

This shock formation and the up-down asymmetry play a part of the L-H transition physics. The up-down asymmetry has influences through gyro-viscosity [34]. The poloidal electric field caused by the non-uniform ion loss is also studied in [100]. As is discussed, the modification of the flow pattern is influential on the transition time scale. The neoclassical ordering is not correct in this regime, and the neoclassical amplification of the dielectric constant can be reduced. This shortens the transition time from the L- state to H-state or vice versa.

The large poloidal flow also influences the MHD equilibrium itself. It has been shown that, if the poloidal flow is large enough, the MHD equilibrium equation (Grad-Shafranov equation) changes its character from elliptic to hyperbolic [101]. The condition for this change of characteristics is expressed for the low β plasma as

$$\frac{V_\theta^2}{v_A^2} \sim \frac{\gamma \mu_0 p}{B^2}$$

where γ is the specific heat ratio here. This criterion is much higher than that for the electric field bifurcation.

6. Improved Confinement

Based on the interactions between the radial electric field and plasma transport coefficient, models explaining the improved confinement have been proposed. First, the H-mode physics is described. Then other types of the improved confinement modes are discussed.

6.1 H-Mode

6.1.1 Bifurcation and Improved Confinement

Equation (50) predicts the bifurcation of the radial electric field. As is pointed out in Eq.(51), there are many nonlinear terms with respect to X (or X') in Eq.(50). A couple of combinations are possible to generate the bifurcation of the solution and to induce the jump of the transport coefficient.

Bifurcation of the hard transition has been found by combining Eq.(50) and (52). First was the analysis on the balance between Γ_{e-i}^{anom} and Γ_i^{ic} [15] and the other was that between Γ_i^{ic} and Γ_i^{bv} [32], predicting the E_r-bifurcation in the H-mode. The variety in the transitions are also noted form Fig.12. Depending on which terms are important in Eq.(51), the direction of the transition changes; either to more positive electric field or more negative one.

The bipolar part of the plasma flux, shown by Eqs.(51), (52) jumps at the critical point as well. The intrinsic-ambipolar component is also reduced. The relations between the transport coefficient with the electric field structure (say, Eq.(40) and others) imply that the transport coefficients for the particles, heat and momentum are subject to the catastrophe simultaneously.

The reduction of the transport coefficient is expressed in Eqs.(37) for quasi-linear estimate or Eqs.(40), (43) for the nonlinear estimate. Fig.16 illustrates the thermal conductivity in the L-phase and H-phase [67]. Strong reduction of the thermal conductivity is demonstrated.

The soft-type transition, as in Fig.10(b), can take place without having the radial electric field bifurcation. If one chooses a picture of the neoclassical theory, i.e., the magnitude of the radial electric field is of the order of T_i'/e, then the electric field shear has the form of [82]

$$S_v \sim -n_i' p_i' / eBn_i^2 \ .$$

If one substitutes this in the assumption Eq.(37), one gets the schematic form like

$$q_{ri} \simeq -\left(C_0 + \frac{C_1}{1 + C_2 (p_i')^2}\right) p_i' \ . \qquad (63)$$

The heat flux can be a decreasing function of the pressure gradient as in Fig.10(b), assuming that C_1 and C_2 are constant. Since this formula is based on a simple approximation of the anomalous transport, the quantitative validity is not conclusive. This result suggests a further possible variety in the improvement of the confinement.

These theoretical results of the L-H transition and the reduced transport (both the hard and soft transition models) are employed in transport simulations. Simulation study is widely performed [102-105]

6.1.2 Threshold Condition

The threshold condition for the bifurcation in the transport coefficient is related to the experimental condition for the onset of the L-H transition. The task is to express the formula of the critical points in Fig.10 (or Fig.11) in terms of the plasma parameters. The importance of the hard type bifurcation has been suggested. In this mechanism, the terms in Eq.(52) play essential roles. The phase diagram associated with the Riemann-Hugoniot catastrophe has been analyzed [24]. The result is not simple but has given several rough estimate for the conditions.

The important role for the ion orbit loss requires the condition

$$\nu_* < \nu_c \sim 1 \ . \qquad (64)$$

The competition between the anomalous transport and the viscous ion loss indicates the condition

$$\lambda_p = \lambda_{pc} \sim \nu_* \rho_p^2 / \hat{D} \ . \qquad (65)$$

The formula (65) was derived in the ordering $\nu_* \rho_p^2/\hat{D} \sim 1$, so that Eq.(65) may be read as

$$\lambda_p \sim 1 \ . \tag{66}$$

The neutral particles are resisting the L-H transition. The upper limit of the neutral density, for the possible L-H bifurcation, was derived as

$$n_0 \leq n_{0c} \sim \frac{\nu_i}{\langle \sigma_{cx} v \rangle} \frac{\rho_p}{\Delta_n} \tag{67}$$

where $\langle \sigma_{cx} v \rangle$ is the charge-exchange cross-section and Δ_n is the penetration length of neutrals. Balancing terms in Eq.(52) simultaneously, the result is found to lie in the range of Eqs.(64)-(66) [106].

The analysis on the experimental threshold condition from the database has been performed to obtain the condition in terms of the operational parameters such as the heating power [107]. The interpretation of the local parameters in the theoretical threshold condition to the operational parameter in experiments requires additional physics, and is not straightforward. Some efforts have been made [108,109]. An encouraging discussion is derived in [109] based on the criterion Eq.(66). However, the theoretical knowledge on the transport in the SoL plasma is still limited [19,110].

The hysteresis nature was studied. Comparing the condition for the back-transition (H-to-L transition) to the L-to-H transition, the hard type bifurcation was obtained [15,32], and was applied to analyze the threshold condition [102].

What has been well-known about the experimental threshold condition was the up-down asymmetry [1,107]. In the tokamak plasma with the poloidal divertor, the threshold power is low if the ion-∇B drift is in the direction of the x-point. Some model predicts that, due to the $E \times B$ drift in the SoL plasma, the edge temperature can be higher in such a condition in comparison with the case of opposite drift [111]. (This would give lower threshold heating power.) However, the numerical simulation has

not necessarily confirmed this dependence of the temperature [112]. Other possibility is the asymmetry of the ion orbit loss with respect to the x-point location. This possibility seems to be not fully analyzed in this context.

The contribution of energetic particles to Eq.(51) is also important problem. The influence of the neutral beam injection or rf-driven energetic particles was studied [113,114]. It has been predicted that these effects are influential even within today's range of the heating power. If the contribution of the alpha-particles, i.e., the fusion product, is taken into account, the additional improvement was predicted [41]. They provide a theoretical prediction for the external control of the confinement improvement.

The study of the threshold condition can also be extended in stellarators and helical systems. The form of Γ_i^{bv} and other terms have different form from those in tokamaks. The comparison with experiments would strengthen the theoretical basis. A model has predicted slower bifurcation [115]. The analysis on Γ_i^{bv} has shown that the bifurcation of the radial electric field occurs at much higher values of X[116].

6.1.3 Transport Barrier

The picture of the interface is extended in the study of the transport barrier of the H-mode. In this case, the plasma parameters, such as the density and temperatures, could change spatially as steep as the transport coefficient or the electric field, and the result is dependent on the boundary condition as well [83]. Figure 17 illustrates the distribution of the transport coefficient near the plasma edge in the L- and H-phase. The meso-phase is formed, and the thickness of the layer is evaluated as

$$\delta \sim \sqrt{\hat{\rho}_p^2 + \mu_\perp / \nu_*} \tag{68}$$

where $\hat{\rho}_p$ is the squeezed poloidal gyro-radius, Eq.(10), and the shear viscosity $\mu_\perp$ is given as Eq.(43). The transport coefficient $\mu_\perp$ is dependent on the radial electric field

shear, i.e., the sharpness of the spatial transition. If the viscosity is reduced, then the interface becomes thinner, and as a consequence of this, the viscosity is further reduced. This system is thus self-organizing the thin transport barrier through the interactions of the electric field and the transport coefficient. Application to the externally- biased limiter is presented in [33], where explicit plasma parameter dependence is incorporated. The analysis on the H-mode plasma is also performed[117].

The transport barrier formation has influence on the global confinement. First, the total stored energy is strongly affected by the height of the pedestal in radial profile [118]. The height of the pedestal is governed by the layer thickness and by the achievable gradient in the barrier. The latter is discussed later in relation with ELMs.

Second, the transport barrier at the edge may affect the transport coefficient in the core. For instance, the edge pedestal elevates the parameters in the core plasma, which at the same time change the transport coefficients in the core. Quantitative analyses has been performed and is presented in the section 6.2.

6.1.4 Limit Cycles and ELMs

Analyses has been done for the system of the evolution equations of plasma parameters, and the limit cycle oscillations were investigated [24,69,71,83,92,93,103]. Solution of this equation and the relation to ELMs [84,119,120] are discussed.

6.1.4.1 Dithering ELMs

The system of dynamical equations of the E-TDGL type, Eq.(56), predicts the limit cycle oscillation, which is the sequence of the transitions and back transitions [83,92,93]. In this analysis, the parameter g, which control the transport, was chosen as

$$g \equiv \frac{\rho_p}{L_n} \frac{\hat{D}_L}{\nu_i \rho_p^2} \tag{69}$$

and N is modelled by the quadratic equation of X. This model is employed by noticing the result that the L-to-H transition occurs if the gradient is sharp and the collisionality is low, i.e., Eqs.(64) and (65). Figure 18 illustrates the limit cycle oscillation seen in the flux out of the plasma. The H-phase and L-phase are realized one by one; in each of the stage, the radial profile of the transport coefficient is those in Fig.17. In the H-phase, the confinement is good so that the increment of the parameter occurs. Owing to this improvement, e.g., the density becomes too high, so that the condition g_m in Fig.11 is reached. Then the sudden increment of the loss rate takes place, causing the jump of the out flux and the rapid decay of the pedestal profile. If the plasma parameter develops, the condition g_M in Fig.11 is realized. Then the transition to the H-phase takes place. These processes repeat themselves. Under the constant supply of the plasma from core, the limit cycle oscillation occurs. This is the self-organized oscillation generated by the hysteresis and hard transition in the plasma transport and the electric field generation. This limit cycle oscillation is possible near by the threshold condition of the L-H transition, which is evaluated in the stationary state [92]. The small and frequent ELMs are observed experimentally in the vicinity of the threshold power for the L-H transition, and is called as dithering ELMs. This limit cycle oscillation constitutes the model of this kind of ELMs.

The appearance of this limit cycle oscillation in the system of Eq.(56) is studied under the slow development of the global plasma parameter [93]. The result is shown in Fig.19. The heat flow from the core is increased gradually in this analysis. It is shown that, as the plasma parameters reaches the threshold condition, the first burst appear, followed by the periodic bursts. As the heating power becomes larger, finally the self-regulated oscillation disappears. The stationary H-mode is established. It is noticed from the figure that the height of the first burst is almost the same as the following one; and the last one is similar to the preceding one. The oscillation

amplitude jumps abruptly from zero to finite value and from finite amplitude to zero. This feature is characteristic to the hard type bifurcation which contains a hysteresis. The shape of each burst must be compared. In the beginning, where the average plasma flux is close to that of L-mode, each period is composed of short and sharp H-state (and long and round L-phase). On the contrary, at the end, the shape of each period is characterized by the short and sharp L-phase. As the heating power becomes larger, then the staying probability in the L-state becomes shorter.

These oscillations can also be found in the zero-dimensional models. If the model takes into account the slow transitions (such as [69,71]) then the gradual appearance of oscillation, rather than the sudden bursting, is predicted at the boundary between the stationary states and oscillating state.

6.1.4.2 Beta-Limit Phenomena

Other types of ELMs has also been found. When the pressure gradient at the edge becomes too high, the ELM burst usually occurs. In the high heating limit, the periodic and giant ELMs are observed, and is called as type-I ELMs. The condition for this burst to occur has been compared to the ideal MHD stability [119]. Under the steep pressure gradient at the edge, high-mode number ideal MHD modes are predicted to become unstable, and the relation with the ELMs has been analyzed (see, e.g.[1]). The catastrophe, which occurs at the critical pressure, occurs periodically; if they happen sequentially, the period for which is expected to be roughly inverse to the heating power. This is in the line of the observations, and the cause of type-I ELMs could be the beta-limiting phenomena. Although the ideal MHD-modes are candidate of the ELMs, the linear theory has its difficulty in explaining the ELMs: This is because, in ELMs, the magnetic perturbations appear very abruptly, and the fast change of the growth rate is beyond what is calculated by the linear theory. Theory of the transport catastrophe and the subsequent periodic bursts have been proposed [121,122]. They

are now applied to the physics of ELMs. Kelvin-Helmholtz instability could also be the origin of the destruction of the H-mode, and investigations has been initiated [123].

The structure of the transport barrier in Fig.17 is thermodynamically stable. If the event happens (by the mechanism such as discussed above), the barrier is destroyed once. However, if the violent instability and transport catastrophe are terminated, then the transport barrier is established again [92]. Transient response of the barrier is shown in Fig.20.

6.2 Other Improved Confinement Modes

The discovery of the H-mode stimulated the finding of the other types of the improved confinement [124]. Some are characterized by the peaking of the profile [125], and for some cases, the transport barrier is formed interior of the plasma [126]. The role of the electric field on such confinement state has also been discussed [19].

6.2.1 Peaked Profile Mode

The peaking of the plasma profile is modelled in terms of the radial electric field [127]. The density peaking without central particle source has been discussed in terms of the inward pinch of particles. For this phenomena, the neoclassical theory [39] as well as the anomalous transport theory has been developed [128], where the growth of the turbulence causes the inward pinch. The off-diagonal terms in Eq.(24) (particularly, the $M_{1,2}$ and $M_{1,3}$ components) contributes to the pinch. The observation, that the pinch becomes prominent as the anomalous transport is reduced, has suggested the role of the radial electric field. Theory of the improved confinement in the peaked profile [127] has pointed out the possibility that the peaked profile of the radial electric field, which is generated by the peaked density, enhances the inward pinch through the anomalous viscosity. Although the diffusion and viscosity reduce together, the balance is shape-dependent, and the peaking is predicted. The reduced neutral density is essential for it, because the neutrals tend to reduce the radial electric

field. This is compared to the nature of the Improved Ohmic Confinement (IOC) which is realized by shut-off the gas puff [125]. An example of the development, associated with the co-and counter NBI heating [129], is shown in Fig.21.

6.2.2 VH-Mode

In the VH mode, the reduction of the transport appear near the edge and in the center simultaneously. When this mode is established in experiments, further reduction of the thermal conductivity happens with the speed-up of the core toroidal rotation. Motivated by this observation, this mode has also been studied along the line of the radial electric field [19,104,130].

The form like Eqs.(43) and (63) was combined with the transport code for the density and temperature. An example of the code, which employs the constant parameters of C_j's in Eq.(63), is reproduced in Fig.22(a) [104]. As the heating power increases, the transport barrier becomes thicker, and the confinement improvement penetrates from the edge to the core; it is established in the wider region. The parallel motion given by the external source is cooperating, and the threshold power is predicted to be smaller in the co-injection case. These results of course depend on the choice of the form Eq.(63). Different parameter dependencies of the coefficients give different answer for the problem [130].

6.2.3 Self-Organization of the Electric and Magnetic Structures

There is an alternate approach for the problem of the VH-mode and related improved-confinement modes. The combined effect of the electric field and the magnetic field structure was pointed out. The form Eq.(43) shows that the strongly-reduced magnetic shear can make the transport coefficient smaller, in addition to the electric field effect. (Mechanisms of the transport reduction in the very low shear has been discussed in, e.g., [65,131].) The increased Shafranov shift and the Bootstrap

current are effective in reducing χ and μ, which cause the enhanced inhomogeneous rotation. The increment in the sheared rotation can then further reduce the transport coefficients, which in turn strengthen the mechanism of the improved confinement. By this link of the mutual interactions, the internal transport barrier was predicted to be established, independent of the edge transport barrier [132]. Example of the result is shown in Fig.22(b). The transport barrier could be established first either at the edge or at the core. The model [132] was also applied to the High-β_p mode or PEP-mode.

7. Discussion on Experimental Observations

Radial Electric Field

The sudden change of the radial electric field at the L-H transition has been found in various circumstances [16]. It is now widely accepted that the sharp layer of the strong electric field is associated with the H-mode transport barrier. A lot of experimental efforts has been paid and the time resolution for the observation has been improved. It has now reached the order of 100 μs in D III-D. Within this time resolution, the development of the radial electric field and the change of the transport occurs together [133]. The multiple transitions (i.e., to that of more positive E_r and to the mode negative E_r) have been confirmed by application of the external radial electric field [134]. Different sign was also found in JT-60 [135].

The working hypothesis of the H-mode, i.e., the electric field bifurcation and associated reduction of the transport, seems, as a whole, to be *not in contradiction* to experimental observations.

Type of Bifurcation

Experiments have shown supports for the picture of the hard transition [93,136]. It has been known that the H-mode could be realized without going through a sharp transition [137.] This latter observation indicates that the soft transition can

also occur. The coexistence of the hard and soft transitions in the cusp type catastrophe, Fig.10(c), works as a basis for the understanding.

Time Scale

The time interval for the jump of the radial electric field in the L-H transition was predicted of the order of $\varepsilon^2 q^{-2} \nu_i^{-1}$ without considering the neoclassical enhancement of the dielectric constant [24]. If one considers the enhancement factor, it would be $\varepsilon^2 \nu_i^{-1}$, which may be slow for the rapid transition [138]. As is discussed in the text, the neoclassical amplification may not appear in the L-H transition. This may indicate the importance of the poloidal variation of the radial flow, i.e., the two-dimensional nature of the transport barrier formation.

Radial Structure

The layer thickness has been experimentally investigated (e.g., [117,139]). The dependence of the layer width on the poloidal gyro-radius has shown to be weak [117]. The theoretical concept like Eq.(68) has not been rejected; but the dependence on the other parameters, e.g., the ion viscosity, has not yet been tested experimentally.

Poloidal Structure

Some experiments has shown the poloidal variation of the profile on the magnetic surface [140]. The formation of the shock has not yet been concluded. The very sharp radial gradient of the plasma profile requires very high accuracy to identify the same magnetic surface at the different poloidal location.

Causality

General observation of the L-H transition and the back transition (H to L-mode) supports the picture of the electric field bifurcation. However, not much quantitative statement could be given on the dominant cause of the L-H transition. Change of the ion loss was observed on JFT-2M [141], showing that the ansatz of the orbit loss is not

excluded. The relation of the various external method and the established radial electric field is investigated [142]: The important role of the non-classical contribution was demonstrated. Direct calculation of the terms in Eq.(51) under the condition of the external bias has given an agreement [33]. The recent observation on the H-mode on stellarator or helical system [143] will provide a further examination for the understanding of the causality in the H-mode. The status is still far from the complete understanding.

Threshold Condition

The comparison in terms of the collisionality has been done. In some cases, rough agreement was seen [133,142], but there still remains discrepancy [144]

The interpretation of the theoretical threshold condition, which is given in the local parameters, into the operational parameter in experiments requires additional physics and is not straightforward. In predicting the threshold condition (like the threshold heating power) based on the conditions (65) and (66), the knowledge of the L-mode transport in the scrape-off-layer plasma is necessary. Thermal conductivity seems close to be the pseudo-classical law in the SoL plasma [145], but requires further experimental progress. Owing to the incompleteness of these knowledge, combined with the uncertainty of the theoretical models, many of the experimental observations on the thresholds condition remain unexplained. Among them, the up-down asymmetry with respect to the x-point location would provide a useful information in the progress.

Reduction of the Transport

The reduction of fluctuations associated with the radial electric field has been widely observed [146]. Experiments have shown that the *observed* mode numbers and amplitude seem to follow the relation like Eq.(34). However, the determination of the mode number and fluctuation level in terms of the plasma parameters is still uncertain.

The impact of the drift reversal on the transport coefficients has been demonstrated clearly in FM-1 [147]. The drift reversal due to the electric field shear, as was predicted in [52], will be studied in future. Another clear demonstration of the fluctuation suppression was observed in mirror experiments [148].

Dynamical Structures

The most prominent in the dynamics of the H-mode is the appearance of the ELMs. The theoretical prediction on the abruptness and the shapes of the bursts features also agrees with experimental observations [120]. The dithering ELMs seem, at least qualitatively, to be explained by the hypothesis of electric field bifurcation of the hard transition type. This provides an experimental basis for the hard transition in the bifurcation.

Giant ELMs are presently investigated intensively, and will be discussed in comparison with experiments in a near future.

An important observation is the burst of the momentum flux in the core plasma, which is called as MTE (Momentum Transfer Events) [149]. After the termination of this event, the VH-mode appears. This waits a theoretical modelling. The clarification of this phenomena would give further progress in understanding of the structural formation and the improved confinement.

Core-Improvement and VH-Mode

The radial electric field in the core has not often been observed. The difference in the E_r profile between the linear-Ohmic Confinement and saturated-Ohmic confinement (SOC) was found [150]. Relation between the SOC-IOC transition needs further experimental study. The study of the peaked density profile on JFT-2M has confirmed the co-esistence of the density peaking and the steep radial electric field [151]. This does not contradict to the theory of mutual sustainment of the peaked profile and large electric field in [127], but the causality has not yet been conclusive. The core-H-mode, driven by the Ion Bernstein mode, was observed [152]. Relation

with the rf-driven poloidal force [87] is discussed; however, the quantitative comparison needs further study.

The development of the confinement improvement in the core will give further test for the theoretical modelling. The theories has provided the pictures that the VH mode transition propagates from the edge [104] or that the internal transport barrier can be established from the inside [132]. The necessary value of E_r' for suppression of the turbulence is intensively tested in experiments [133]. Future detailed observation will give detailed comparison.

The observation on the change of the q(r) profile prior to the appearance of the VH-mode [153] suggests the importance of the cooperation of the magnetic structure for the reduced transport in the core and for the change in other improved confinement modes [154].

Pinch, Spontaneous Drive and Propagation

The effects of various gradients on the electric field generation have been studied intensively. At the same time, the study on the plasma flux (pinch terms) caused by the electric field is the corresponding key issue. Spontaneous torque was very recently identified experimentally [155]. In parallel with the comparison of the transport coefficient Eq.(43) with experiments, the future study on the parameter dependence of this torque could be compared to the theory Eq.(48). Experimentally, there is a clear evidence of the existence of the heat flow in the direction of higher temperature direction [156]. This waits further theoretical progress as well.

The change of transport in the core is often considered as a consequence of the change in the plasma parameter, so that this variation propagates into the core with the time scale of the confinement time. In addition to this kind of slow propagation of change, there is possibly a fast propagation of change into the core plasma after the L-H transition [157]. Similar fast propagation of the change of the transport coefficient has been observed within the transient responses (e.g., the pellet injection, sawtooth, X-

events, etc. [158]. In order to model this kind of fast propagation, some models have been proposed, based on the avalanche of bifurcation [159].

Atomic and Molecular Physics

Also important in the process of the electric field and confinement are the atomic physics and plasma wall interactions. Difference of the confinement due to the wall material has been reported. Some of the atomic physics has been modelled [160,161]. For instance, the influence of the wall material was formulated in terms of the reflected neutral particles [160]. Impact of the neutral particles [24,86] has to be compared to experimental result [162]. Role of Z_{eff} on the bifurcation was discussed [163]. The necessity of the low Z_{eff} value has also been pointed out for the VH-mode in experiments [164]. Combined with the fact that the first VH mode appeared after Boronization in D III-D [165], the important role of atomic physics is implied. There still remains a big mystery about the isotopic effect on the improved confinement factor [1]. The H-mode in the DT plasma has also illustrated this problem, by showing a better confinement than the H-mode in the DD plasma [166]. The heavier neutrals (T) penetrate less than the lighter neutrals (D) and the neutral density in the transport barrier could be lower in the DT plasma. The theory predicts the improvement through this mechanism. This agrees with observation qualitatively, but the quantitative analysis has not been given. These observations suggest the necessary future theoretical study .

8. Summary

In this article, we reviewed the recent theoretical progress on the role of radial electric field on toroidal confinement. The study on the electric field effect, motivated by the finding of the improved confinement in tokamaks, has flourished these years. This is partly because the main hypothesis, i.e., the electric field bifurcation and reduced transport, has shown some success in explaining various aspects of the complex observations of the H-mode. It is also because, through the investigation of

the dynamic phenomena in improved confinement modes, the theory has provided a clear example of the physics of the structural formation in the nonlinear and non-equilibrium media. This has given new enlightenment on the long-lasting challenge in the plasma confinement; the anomalous transport. This review has put emphasis on the research in this direction.

In this review it is intended to clarify the physics considerations on the electric field effect on the confinement and the structural formation in the plasma. It also tries to illuminate how the collaborative and interactive communication with experiments has been fruitful for theoretical progress. At present, the working hypothesis of the H-mode based on the electric field bifurcation seems, as a whole, to be *not in contradiction* to experimental observations. It would be surprising that, in such important and complex situation like the H-mode, the prediction of the role of electric field has obtained the experimental supports (and survived the tests).

A few detailed points and future problems are seen here.

This article covers mainly on torus plasmas. However, the physics picture could be valid and will be enriched if applied to wider circumstances. A similar phenomena of the confinement improvement have also been observed on mirror devises [167,168]. The fluctuation level varies as the change of the radial electric field. It is conjectured that the radial transport of the core plasma in the mirror is in a state similar to the H-mode of a tokamak. The bifurcation has also been induced by the biased probe [167]. The coupling of the radial electric field to the parallel electric field should be strong in mirrors, and anisotropy of the distribution would introduce the additional physics for the electric field generation. Not the identical theory would apply, but much similarity is found, like the modification of the orbit loss by the electric field. In particular, they will give a impact on the simultaneous study of the two-dimensional electric field structure. The theoretical study of the electric field effect on the confinement has helped the emerging trend that the various toroidal configurations are analyzed by an unified physics picture. The extension of this unification to the wider circumstances will be prosperous.

In relation to the topics of this article, lots of work were not properly discussed here. The contact surface between of the regions of the different magnetic topologies is an important issue for the electric field effect [25,169,170]. One is the problem of the radial electric field right at the surface. The closed magnetic surfaces are separated from the open field lines by the separatrix. The scale length of the radial sheath and the connection with the SoL plasma has been discussed [25,170]. The other is the interface between the closed magnetic surface and the braided magnetic surface [169]. The magnetic braiding selectively increases the average electron loss, and the term Eq.(52-1) with proper choice of diffusivity [171] becomes dominant. The solution of Eq.(50) is different from that of the closed surfaces (see e.g., [172,173]). This can cause a strong shear of electric field in the side of the closed magnetic surfaces. The improvement of the confinement is expected. Some experiments have indicated the important role of the magnetic structure in the H-mode [174]. The complex plasma dynamics through the magnetic structure has been well known [175], and the analysis coupled with the electric field is not developed well.

To make the physics picture of the electric field and confinement more complete, the future theoretical studies will be extended in the following directions;

1: Bifurcation physics
2: Turbulent transport
3: Collisional transport
4: Geometrical effects (including SoL)
5: Transients and stationary states
6: Catastrophic events
7: Physics of impure plasmas.

Viewing these points, by which the theory of the improved confinement will be propelled, one may realize that the understanding of the role of the electric field in confinement is almost equivalent to understanding of the magnetic confinement itself.

Acknowledgements

Authors cordially acknowledge Dr. A. Fukuyama for collaboration and enlightenment on the problem. They wish to thank many of authors of the quoted articles for useful discussions, to which this review owes much. In particular, they are grateful Prof. F. Wagner and Prof. K. Lackner and ASDEX Team and Wendelstein 7AS Group, Dr. K. H. Burrell and Doublet III-D Group, Dr. K. Ida and JIPP T-IIU Group and CHS Group, Dr. Y. Miura, late Prof. H. Maeda and JFT-2M Group, Dr. M. Azumi and JT-60 Group, Dr. M. Keilhacker and JET Team, Dr. H. Zohm and ASDEX-U Team, Dr. H. Zushi and Heliotron-E Group, Dr. C. E. Bush and TFTR Group, Prof. G. H. Wolf and TEXTOR Group, and members of the ITER H-mode database for discussion on the experimental data. Thanks are also due to Prof. T. Ohkawa, Dr. H. Sanuki, Dr. K. C. Shaing, Dr. F. L. Hinton, and Prof. M. Wakatani for discussion on the problem.

This work is partly supported by the Grant-in-Aid for Scientific Research of Ministry of education and by the Collaboration programme of Advanced Fusion Center of Kyushu University.

This article is dedicated to Prof. S. Yoshikawa on occasion of his sixtieth birthday.

References

[1] Wagner F et al 1982 *Phys. Rev. Lett.* **49** 1408.

ASDEX Team 1989 *Nucl Fusion* **29** 1959.

[2] Miyamoto K 1976 *Plasma Physics for Nuclear Fusion* (Iwanami, Tokyo) (English Translation, MIT Press 1980) .

[3] Timofeev A V 1992 in *Reviews of Plasma Physics* (Consultants Bureau, New York) Vol. 17, p193.

[4] Kovrizhnykh L M 1984 *Nuclear Fusion* **24** 851.

[5] Davidson R C 1974 *Theory of Non Neutral Plasma* (Benjamin, Reading)

[6] Budker G I 1961 in *Plasma Physics and Problems of Controlled Thermonuclear Reaction* (ed M A Leontovich, New York, Pergamon Press) Vol.1, 78.

[7] Baity F W et al 1983 in *Plasma Physics and Controlled Nuclear Fusion Research 1982* (IAEA, Vienna) Vol.2, p185.

Ikegami H et al 1987 in *Plasma Physics and Controlled Nuclear Fusion Research 1986* (IAEA, Vienna) Vol.2, p489.

[8] Hinton F L, Hazeltine R D 1976 *Rev. Modern Phys.* **48** 239.

Hirshman S P, Sigmar D J 1981 *Nucl. Fusion* **21** 1079.

[9] Connor J W, Hastie R J 1971 *Phys. Fluids* **17** 114.

Galeev A A and Sagdeev R Z 1977 *Review of Plasma Physics*, ed M. A. Leontovich (Consultants Bureau, New York) Vol.7, 307.

Potok P E, Politzer P A, Lidsky L M 1980 *Phys. Rev. Lett.* **45** 1328.

Boozer A H Kuo-Petravic G 1981 *Phys. Fluids* **24** 851

Hastings D E 1984 *Phys. Fluids* **27** 939.

[10] Pastukov V P 1987 in *Reviews of Plasma Physics* (Consultants Bureau, New York) Vol. 13, 203.

[11] Dimov G I, Zakaidakov V V, Kishinevskii M E 1976 *Sov. J. Plasma Phys.* **2** 326 [*Fiz. Plazmy* **2** 597].

Fowler T K, Logan B G 1977 *Comments Plasma Phys. Contr. Fusion* **2** 167.

[12] Furth H P 1975 *Nucl. Fusion* **15** 487.

[13] Crowley T P, Rensselaer Plasma Dynamic Laboratory Team 1994 *IEEE Trans. Plasma Science* **22** 291.

Dnestrovskij Yu N, Melnikov A V, Krupnik L I, Nedelskij I S 1994 *IEEE Trans. Plasma Science* **22** 310.

[14] Ohkawa T, Hinton F L, Liu C S, Lee Y C 1983 *Phys. Rev. Lett.* **51** 2102

[15] Itoh S-I, Itoh K 1988 *Phys. Rev. Lett.* **60** 2276.

[16] Groebner R J, Burrell K H, Seraydarian 1990 *Phys. Rev. Lett.* **64** 3015.

Ida K, Hidekuma S, Miura Y, Fujita T, Mori M, Hoshino K, Suzuki N, Yamauchi T, JFT-2M Group 1990 *Phys. Rev. Lett.* **65** 1364.

[17] Wobig H, Maassberg H, Renner H, WVII-A Team, ECH Group, NI Group 1987 in *Plasma Physics and Controlled Nuclear Fusion Research 1986* (IAEA, Vienna) Vol.2, p369.

[18] Itoh K 1994 *Plasma Phys. Contr. Fusion* **36** A376.

[19] For a review on this subject see, e.g.,

Itoh K, Itoh S-I, Sanuki H, Fukuyama A 1994 *IEEE Trans. Plasma Science* **22** 376.

Itoh S-I, Itoh K, Fukuyama A 1995 *J. Nucl. Materials* **220-222** 117.

[20] Mikhailovskii A B 1992 *Electromagnetic instibilities in an inhomogeneous plasma* (IOP Publishing, Bristol)

[21] Itoh K, Sanuki H, Itoh S-I, Tani K 1991 *Nucl. Fusion* **31** 1405.

[22] Nishitani T, Tobita K, Tani K et al. 1993 in *Plasma Physics and Controlled Nuclear Fusion Research 1992* (IAEA, Vienna) Vol.1, p.351.

[23] Mynick H E 1983 *Phys. Fluids* **26** 1008.

[24] Itoh S-I, Itoh K 1989 *Nucl. Fusin* **29** 1031.

[25] Hazeltine R D 1989 *Phys. Fluids B* **1** 2031.

Hinton F L 1987 presented in Sherwood Theory Meeting (Oak Reidge, TN)

[26] Itoh S-I, Itoh K, Ohkawa T, Ueda N 1989 in *Plasma Physics and Controlled Nuclear Fusion Research 1988* (IAEA, Vienna) Vol.2, p23.

[27] Miyamoto K 1994 *J. Plasma Fusion Research* **70** 882.

Chankin A V, McCracken G M 1993 *Nucl. Fusion* **33** 1459.

[28] Itoh K, Sanuki H, Todoroki J, et al. 1991 *Phys. Fluids* B **3** 1294.

[29] Ichimaru S 1973 *Basic Principles of Plasma Physics* (Benjanim, Reading)

[30] Kaufman A N 1958 *Phys. Fluids* **1** 252.

[31] Galeev A A, Sagdeev R Z 1968 *Sov. Phys. JETP* **26** 233. [*Zh. Eksp. Teor. Fiz.* **53**, 348 (1967).]

Stringer T E, Connor J W 1971 *Phys. Fluids* **14** 2177.

Stix T H 1973 *Phys. Fluids* **16** 1260.

Hazeltine R D, Ware A A 1978 *Plasma Phys.* **20** 673.

[32] Shaing K C, Crume E Jr. 1989 *Phys. Rev. Lett.* **63** 2369.

[33] Stringer T E 1993 *Nucl. Fusion* **33** 1249.

[34] Stacy W M 1989 *Plasma Phys. Contr. Fusion* **31** 1468

--- 1993 *Phys. Fluids* B **5** 1413.

Connor J W, Cowley S C, Hastie R J, Pan L R 1987 *Plasma Phys. Contr. Fusion* **29** 931.

[35] Hinton F L, Wong S K 1985 *Phys. Fluids* **28** 3082.

[36] Shaing K C, Hsu C T, Hazeltine R D 1994 *Phys. Plasmas* **1** 3365.

[37] Hirshman S P, Shaing K C, van Rij W I, Beasley C O, Crume E C Jr. 1986 *Phys. Fluids* **29** 2951.

Garabedian P R 1994 *Communications on Pure Appl. Math.* **XLVII** 281.

[38] Bickerton R J, Connor J W, Taylor J B 1971 *Nature Physical Science* **229** 110.

[39] Ware A A 1970 *Phys. Rev. Lett.* **25** 15.

[40] Nakajima N, Okamoto M 1992 *J. Phys. Soc. Jpn.* **61** 833.

Nakajima 1993 presented at Annual Meeting of Phys. Soc. Jpn.

[41] Ohkawa T 1994 *Comments Plasma Phys. Contr. Fusion* **16** 1.

[42] Yoshikawa S 1980 "*Impurity Ions in a Rotating Tokamak*", Res. Rep. PPPL-1710, Princeton Univ.

[43] Kadomtsev B B 1965 *Plasma Turbulence* (Academic Press, New York)

[44] Yoshikawa S 1970 in *Methods of Experimental Physics* (Ed. Griem H R, Loveberg R H, Academic Press, New York) Vol.9, Chapter 8.
Liewer P 1985 *Nucl. Fusion* **25** 543.

[45] Wagner F, Stroth U 1993 *Plasma Phys. Contr. Fusion* **35** 1321.

[46] Pearlstein L D, Berk H L 1968 *Phys. Rev. Lett.* **23** 220.

[47] Inoue S, Tange T, Itoh K, Tuda T, 1979 *Nucl. Fusion* **19** 1252.
Horton C W 1980 *Plasma Phys.* **22** 345
Waltz R E 1982 *Phys. Fluids* **25** 1269.

[48] Barescu R 1991 *Phys. Fluids B* **3** 564.
Hazeltine R D, Mahajan S M, Hitchcock D A 1981 *Phys. Fluids* **24** 1164.
Shaing K C 1988 *Phys. Fluids* **31** 2249.
Itoh S-I 1992 *Phys. Fluids B* **4** 796.

[49] Sanuki H 1984 *Phys. Fluids* **27** 2500.

[50] See, e.g.,
Lehnert B 1966 *Phys. Fluids* **9** 1367.

[51] Hassam A B 1991 *Comments Plasma Phys. Contr. Fusion* **14** 275.
Shaing K C 1991 *Comments Plasma Phys. Contr. Fusion* **14** 41.

[52] Itoh S-I, Itoh K 1990 *J. Phys. Soc. Jpn.* **59** 3815.

[53] Shaing K C et al. 1989 in *Plasma Physics and Controlled Nuclear Fusion Research 1988* (IAEA, Vienna) Vol.2, p13.
Shaing K C, Crume E C Jr, Houlberg W A 1990 *Phys. Fluids B* **2** 1492.

[54] Biglari H, Diamond P H, Terry P W 1990 *Phys. Fluids B* **2** 1.

[55] Zhang Y Z, Mahajan S M 1992 *Phys. Fluids B* **4** 1385.

[56] Hirshman S P, Molvig K 1979 *Phys. Rev. Lett.* **42** 648.

[57] Wakatani M, Watanabe K, Sugama H, Hasegawa A 1992 *Phys. Fluids B* **4** 1754.

[58] Carreras B A, Sidikman K, Diamaond P H, Terry P W, Garcia L 1992 *Phys. Fluids B* **4** 3115.

[59] Onuki A, Kawasaki K 1979 *Ann. Phys.* **121** 456.

[60] Taylor G I 1934 *Proc. R. Soc. London* **A146** 501.

[61] Lord Rayleigh 1914 *Phil. Mag.* **34** 94.

For recent review, see, e.g.,

Mel'nikov V I 1991 *Phys. Rep.* **209** 1.

[62] Connor J W, Maddison G P, Wilson H R, Corrigan G, Stringer T E, Tibone F 1993 *Plasma Phys. Contr. Fusion* **35** 319.

[63] Ross D W, Mahajan S M 1978 *Phys. Rev. Lett.* **40** 324.

Tsang K T, Catto P J, Whitson J C, Smith J 1978 *Phys. Rev. Lett.* **40** 327.

[64] Scott B D 1990 *Phys. Rev. Lett.* **65** 3289.

Carreras B A, Lynch V E, Garcia L, Diamond P H 1992 *Phys. Fluids B* **5** 1491.

[65] Itoh K, Itoh S-I, Fukuyama A 1992 *Phys. Rev. Lett.* **69** 1050.

Itoh K, Itoh S-I, Fukuyama A, Yagi M, Azumi M 1994 *Plasma Phys. Contr. Fusion* **36** 279, 1501.

Yagi M, Itoh K, Itoh S-I, Fukyama A, Azumi M 1994 *J. Phys. Soc. Jpn.* **63** 10.

See also Connor J W 1993 *Plasma Phys. Contr. Fusion* **35** 757.

[66] Itoh K, Itoh S-I, Fukuyama A, Sanuki H, Yagi M 1994 *Plasma Phys. Contr. Fusion* **36** 123.

[67] Itoh S-I, Itoh K, Fukuyama A, Yagi M 1994 *Phys. Rev. Lett.* **72** 1200.

[68] Hasegawa A, Mima K 1977 *Phys. Rev. Lett.* **39** 205.

Hasegawa A 1985 *Adv. Phys.* **34** 1

[69] Diamond P H, Liang Y-M, Carreras B A, Terry P W 1994 *Phys. Rev. Lett.* **72** 2565.

[70] Drake J F, et al 1992 *Phys. Fluids B* **4** 488.

[71] Rohzanskii V, Tendler M 1992 *Phys. Fluids B* **4** 1877.

Sugama H, Horton C W 1995 *Plasma Phys. Contr. Fusion* **37** 345.

[72] Drake J F, Antonsen T M, Finn J M, et al. 1993 in *Plasma Physics and Controlled Nuclear Fusion Research 1992* (IAEA, Vienna) Vol.2, p115.

[73] Stringer T E 1969 *Phys. Rev. Lett.* **22** 1770.

[74] See, e.g.,

Ruediger G 1989 *Differential Rotation and Stellar Convection* (Gordon and Breach, New York)

[75] Hasegawa A, Wakatani M 1987 *Phys. Rev. Lett.* **59** 1581.

Sugama H, Wakatani M, Hasegawa A 1988 *Phys. Fluids* **31** 1601.

[76] Itoh K, Itoh S-I, Fukuyama A, Yagi M 1995 *'On the Minimum Circulating Power of Steady State Tokamaks'* (preprint, NIFS)

[77] Itoh S-I, Itoh K 1988 *Phys. Letters* **A 127** 267.

[78] Yoshizawa A 1991 *Phys. Fluids B* **3** 2723.

[79] Yoshizawa A 1990 *Phys. Fluids B* **2** 1589.

Yoshizawa A, Yokoi N 1993 *Astrophys. J* **407** 540.

[80] See, e.g.,

Landau L D, Lifshitz I M 1959 in *Corse of Theoretical Physics*, Vol.5: *Statistical Physics* (Pergamon Press, London).

Haken H 1976 *Synergetics* (Springer Verlag, Berlin).

[81] Sanuki H et al. 1995 *Physica Scripta* **51** No.6 in press.

[82] Hinton F L 1991 *Phys. Fluids B* **3** 696.

[83] Itoh S-I, Itoh K, Fukuyama A, Miura Y 1991 *Phys. Rev. Lett.* **67** 2485.

[84] Keilhacker M et al. 1984 *Plasma Phys. Contr. Fusion* **26** 49.

Gohil P, et al. 1988 *Phys. Rev. Lett.* **61** 1603.

[85] See, e.g.,

Tominaga H, Mori H 1994 *Prog. Theor. Phys.* **91** 1081.

[86] Ohkawa T, Hinton F L 1987 in *Plasma Physics and Controlled Nuclear Fusion Research 1986* (IAEA, Vienna) Vol.2, p221.

[87] Inoue S, Itoh K 1981 in *Plasma Physics and Controlled Nuclear Fusion Research 1980* (IAEA, Vienna) Vol.II, p649.
Craddock G G, Diamond P H 1991, *Phys. Rev. Lett.* **67** 1535.
Qiu X M, Bai L, Ran L B 1993 in *Plasma Physics and Controlled Nuclear Fusion Research 1992* (IAEA, Vienna) Vol.2, p.269.

[88] Fried B D, Conte S D 1961 *The Plasma Dispersion Function* (Academic Press, New York)

[89] Shaing K C, Hazaltine R D, Sanuki H 1992 *Phys. Fluids B* **4** 404.

[90] Hirshman S P 1978 *Nucl. Fusion* **18** 917.
---- 1978 *Phys. Fluids* **21** 1295.
Hinton F L, Robertson 1984 *Phys. Fluids* **27** 1243.

[91] Wobig H 1994 '*Stationary equilibrium and Rotation in a Collisional Plasma in a Torus*' (IPP 2/322, Max-Planck-Institute fur Plasmaphysik)

[92] Itoh S-I, Itoh K, Fukuyama A 1993 *Nucl. Fusion* **33** 1445.

[93] Zohm H 1994 *Phys. Rev. Lett.* **72** 222.

[94] Hastings D E, Hazeltine R D, Morrison P J 1986 *Phys. Fluids* **29** 69.

[95] Yahagi E Itoh K, Wakatani M 1988 *Plasma Phys. Contr. Fusion* **30** 1009.

[96] Shaing K C 1984 *Phys. Fluids* **27** 1567.

[97] Haken H 1976 *Synergetics* (Springer Verlag, Berlin) Section 9.3.

[98] Hazeltine R D, Lee E P, Rosenbluth M N 1971 *Phys. Fluids* **14** 361.
Greene J M, Johnson J L, Weimer K E, Winsor N K 1971 *Phys. Fluids* **14** 1258.

[99] Taniuti T, Miriguchi H, Ishii Y, Watanabe K, Wakatani M 1992 *J. Phys. Soc. Jpn.* **61** 568.

[100] Tendler M, Daybelge U, Rozhansky R 1993 in *Plasma Physics and Controlled Nuclear Fusion Research 1992* (IAEA, Vienna) Vol.2, p.243.
Xiao H, Hazeltine R D, Valanju P M 1994 *Phys. Plasmas* **1** 3641.

[101] Zehrfeld H P, Green B J 1972 *Nucl. Fusion* **12** 529.
Hameiri E 1983 *Phys. Fluids* **26** 230.
Kerner W, Tokuda S 1987 *Z. Naturf. a* **42** 1154.
Zelazny R, Stankiewicz R, Galkowski A, Potempski S 1993 *Plasma Phys. Contr. Fusion* **35** 1215.

[102] Shimizu K, Hirayama T, Shirai H, Azumi M, JT-60 Team 1989 *J. Nucl. Mater.* **162-164** 612.

[103] Drestrovskij A Yu, Parail V V, Vojtsenkhhovich I A 1993 in *Plasma Physics and Controlled Nuclear Fusion Research 1992* (IAEA, Vienna) Vol.2, p.371.

[104] Hinton F L, Staebler G M 1993 *Phys. Fluids B* **5** 1281.
Hinton F L, Staebler G M, Kim Y-B 1994 *Plasma Phys. Contr. Fusion* **36** A237.

[105] Fukuyama A, Fuji Y, Itoh K, Itoh S-I 1994 *Plasma Phys. Contr. Fusion* **36** A159.

[106] Toda S, Itoh S-I, Kubota T, Yamaguchi H, Fukuyama A, Itoh K 1995 *Trans. Fusion Tech.* **27** 489.

[107] Kardaun O J W F et al. 1993 in *Plasma Physics and Controlled Nuclear Fusion Research 1992* (IAEA, Vienna) Vol.3, p251.
Ryter F et al. 1993 in *Proc. 20th EPS Conf. on Controlled Fusion and Plasma Physics* (Lisboa) Vol.17C, Part I, p.15.

[108] Itoh K, Itoh S-I 1989 *Plasma Phys. Contr. Fusion* **31** 487.

[109] Cordey J G, Kerner W, Pogutse O, 1994 *'Dimensionless Form of for the L-H Power Threshold'* JET-P(94)66 (preprint).

[110] Stangeby P C, McCracken G M 1990 *Nucl. Fusion* **30** 1035.

[111] Hinton F L, Staebler G M 1989 *Nucl. Fusion* **29** 405.

[112] Ueda N et al. 1994 *Contrib. Plasma Phys.* **34** 350.

[113] Ohkawa T, Miller R L 1991 in *Plasma Physics and Controlled Nuclear Fusion Research 1990* (IAEA, Vienna) Vol.1, p.585.

[114] Itoh K, Itoh S-I 1992 *Nucl. Fusion* **32** 2243.

Yushmanov P N, Dong J Q, Horton W, Su X N, Krasheninnikov S I 1994 *Phys. Plasmas* **1** 1583.

Matsuoka M, Takamura S 1993 *Nucl. Fusion* **33** 161

[115] Itoh K, Itoh S-I, Sanuki H, Fukuyama A 1992 *Comments Plasma Phys. Contr. Fusion* **14** 343.

[116] Shaing K C, Hsu C T, Christenson P J 1994 *Plasma Phys. Contr. Fusion* **36** A75.

[117] Ida K et al 1994 *Phys. Fluids B* **4** 2200.

[118] JET Team (presented by Keilhacker M) 1989 in *Plasma Physics and Controlled Nuclear Fusion Research 1988* (IAEA, Vienna) Vol.1, p.159.

[119] Burrell K H, Allen S L, Bramson G, Brooks N H, Callis R W, Carlstrom T N, et al. 1989 in *Plasma Physics and Controlled Nuclear Fusion Research 1988* (IAEA, Vienna) Vol.1, p.193.

Zohm H et al. 1992 *Nucl. Fusion* **32** 489.

[120] Zohm H, Suttrop W, Buchl K, de Blank H J, Gruber O, et al. 1995 *Plasma Phys. Contr. Fusion* **37** 437.

[121] Itoh K, Itoh S-I, Fukuyama A 1995 *Plasma Phys. Contr. Fusion* **37** in press.

[122] Haas F A, Thyagaraja A 1995 *Plasma Phys. Contr. Fusion* **37** 415.

[123] Itoh S-I, Itoh, K 1987 IPP III/126 (Max-Planck-Institute fur Plasmaphysik)

Chiuch T, Terry P W, Diamond P H, Seddack J E 1986 *Phys. Fluids* **29** 231.

[124] See a review, e.g.,

Stambaough R D et al. 1990 *Phys. Fluids B* **2** 2941.

[125] Soeldner F X et al. 1988 *Phys. Rev. Lett.* **61** 1105.

Fussmann G, et al. 1989 in *Plasma Physics and Controlled Nuclear Fusion Research 1988* (IAEA, Vienna) Vol.1, p.145.

[126] Simonen T C, Matsuoka M, Bhadra D K, Burrell K H, Callis R W et al. 1988 *Phys. Rev. Lett.* **61** 1720.

Koide Y, Kikuchi M, Ishida S, Mori M, Tsuji S, et al. 1994 *Plasma Phys. Contr. Fusion* **36** A195.

[127] Itoh S.-I. 1990 *J. Phys. Soc. Jpn.* **59** 3431.

[128] Coppi B, Spight C 1978 *Phys. Rev. Lett.* **41** 551.

Antonsen T, Coppi B, Englage R 1979 *Nucl. Fusion* **19** 641.

[129] Fukuyama A, Fuji Y, Itoh K, Itoh S-I 1994 *Plasma Phys. Contr. Fusion* **36** A159.

[130] Shaing K C 1994 *Phys. Plasmas* **1** 219.

[131] Kadomtsev B B Pogutse O P 1970 in *Review of Plasma Physics* (Consultants Bureau, New York) Vol.5

[132] Fukuyama A, Itoh K, Itoh S-I, Yagi M, Azumi M 1994 *Plasma Phys. Contr. Fusion* **36** 1385.

[133] Burrell K H 1994 *Plasma Phys. Contr. Fusion* **36** A291.

Burrell K H et al. 1992 *Plasma Phys. Contr. Fusion* **34** 1859.

[134] Weynants R R, et al. 1992 *Nucl. Fusion* **32** 837.

Taylor R J, Brown M L, Fried B D, Brote H, Liberati J R, et al. 1989 *Phys. Rev. Lett.* **63** 2365.

Sasaki S, Uesugi Y, Takamura S, Sanuki H, Kadota K 1994 *Phys. Plasmas* **1** 1089.

[135] Tsuji S 1993 (private communications)

[136] Holzhauer E, et al 1994 *Plasma Phys. Contr. Fusion* **36** A3.

[137] See, e.g.,

Kameari A, Konoshima S, Abe M, Itoh K, Kitsunezaki A, et al. 1987 *Jpn. J. Appl. Phys.* **26** 598.

[138] Hugill J 1994 *Plasma Phys. Contr. Fusion* **36** B173.

[139] Kikuchi M et al 1993 in *Plasma Physics and Controlled Nuclear Fusion Research 1992* (IAEA, Vienna) Vol.1 p.189.

[140] Taylor R J, Pribyl P, Tynan G R, Wells B C, 1994 *Plasma Phys. Contr. Fusion* **36** A105.

---- 1995 in *Plasma Physics and Controlled Nuclear Fusion Research 1994* (IAEA, Vienna) paper A-2/4-P-16.

[141] Miura Y et al 1992 *Phys. Rev. Lett.* **69** 2216.

[142] Ida K et al. 1994 *J. Plasma Fusion Research* **70** 514 (in Japanese).

[143] Toi K et al 1993 in *Plasma Physics and Controlled Nuclear Fusion Research 1992* (IAEA, Vienna) Vol.2, p461.

Erkmann V et al 1993 in *Plasma Physics and Controlled Nuclear Fusion Research 1992* (IAEA, Vienna) Vol.2, p.469.

---- 1993 Phys. Rev. Lett. **70** 2086.

Zushi H, Nagasaki K, Mizuuchi T, Kondo K, Takada H, et al. 1994 *Plasma Phys. Contr. Fusion* **36** 231.

[144] Fukuda T, Kikuchi M, Koide Y, Sato M, Neyatani Y, Azumi M 1994 *Plasma Phys. Contr. Fusion* **36** A87.

[145] McCormick K et al. 1992 *J Nucl. Mater.* **196-198** 264.

Endler M, Giannone K, McCormick K, Niedemeyer H, Rudyj A, et al. 1994 in *Proc. 21th EPS Conf. on Controlled Fusion and Plasma Physics* (Montpellier) Vol.18B, Part II, p.874

Itoh S-I, Itoh K 1994 *Plasma Phys. Contr. Fusion* **36** 1845.

[146] Ritz Ch P, Lin H, Rhodes T L, Wootton A J, 1990 *Phys. Rev. Lett.* **65** 2543.

Couture P, Boileau A, Decoste R, Gregory B, Janiki C et al. 1992 *Phys. Lett.* **A 163** 204.

Doyle E J et al. 1993 in *Plasma Physics and Controlled Nuclear Fusion Research 1992* (IAEA, Vienna) Vol.1, p235.

Ohdachi S, Sgoji T, Nagashima K, Tamai H, Miura Y, Maeda H, Toyama H, JFT-2M Group 1994 *Plasma Phys. Contr. Fusion* **36** A201.

[147] Yoshikawa S 1973 *Nucl. Fusion* **13** 433.

[148] Mase A, Itakura A, Inukate M, Ishii K, Jeong J H, et al. 1991 *Nucl. Fusion* **31** 1725.

[149] Osborne T H 1993 (private communications) presented at *US-Japn Workshop on Transient Phenomena in Toroidal Plasmas* (Sana Diego): See also Osborne T H et al. 1994 *Plasma Phys. Contr. Fusion* **36** A237.

[150] Bugarya V I, Gorshkov A V, Grashin S A et al. 1983 *JETP Lett.* **38** 404 [*Pisma Zh. Eksp. Teor. Fiz.* **38** 337.]
Bugarya V I, Gorshkov A V, Grashin S A, Ivanov I V, Krupin V A, et al. 1985 *Nucl. Fusion* **25** 1707.

[151] Ida K, et al. 1992 *Phys. Rev. Lett.* **68** 182.

[152] Kaita R, Asakura N, Batha S H, Bell R E, Bernabei S, et al. 1993 in *Plasma Physics and Controlled Nuclear Fusion Research 1992* (IAEA, Vienna) Vol.1, p.635.

[153] Lazarus E A, Hyatt A W, Osborne T H, Attenberger S E, Austin M E, et al. 1995 in *Plasma Physics and Controlled Nuclear Fusion Research 1994* (IAEA, Vienna) paper A-5-I-1.

[154] See, e.g.,
Goldston R J et al. 1994 *Plasma Phys. Contr. Fusion* **36** B213.

[155] Ida K, Miura Y, Matsuda T, Itoh K, Hidekuma S, Itoh S-I, JFT-2M Group 1995 *Phys. Rev. Lett.* **74** 1990.
Nagashima K, Koide Y, Shirai H 1994 *Nucl. Fusion* **34** 449.

[156] Luce T C, Petty C C, deHaas J C M 1992 *Phys. Rev. Lett.* **68** 52.

[157] Neudatchin S V, Cordey J G, Muir D G 1993 in *Proc. 20th EPS Conf. on Controlled Fusion and Plasma Physics* (Lisboa) Vol.17C, Part I, p.83.
Cordey J G, Muir D G, Neudatchin S V, Parail V V, Ali-Arshad S, et al. 1994 *Plasma Phys. Contr. Fusion* **36** A267.

[158] Sakamoto M, Sato K N, Ogawa Y, Kawahata K, Hirokura S, et al. 1991 *Plasma Phys. Contr. Fusion* **33** 583.
Frederickson E D, McGuire K, Cavallo A, Budny R, Janos A, Monticello D, et al. 1990 *Phys. Rev. Lett.* **65** 2869.

[159] Kadomtsev B B, Itoh K, Itoh S-I 1995 *Comments Plasma Phys. Contr. Fusion* **17** in press.
Diamond P H, Hahm T S 1995 '*On the Dynamics of Turbulent Transport Near Marginal Stability*' (preprint)

[160] Itoh K, Itoh S-I 1995 *Plasma Phys. Contr. Fusion* **37** 491.

[161] Rogister A L 1994 *Plasma Phys. Contr. Fusion* **36** A219.

[162] Miura Y, Takizuka T, Tamai H, Matsuda T, Suzuki N, et al. 1992 *Nucl. Fusion* **32** 1473.

[163] Ohkawa T, Itoh K, Itoh S-I 1988 *Kakuyugou Kenkyu* **59** 488.

[164] Konoshima S et al 1993 *Bull. Amer. Phys. Soc.* **38** 2062.

[165] Jackson G L et al 1991 *Phys. Rev. Lett.* **67** 3098.

[166] Hawryluk R J et al. 1995 in *Plasma Physics and Controlled Nuclear Fusion Research 1994* (IAEA, Vienna) paper A-1-I-1.

Bush C E, et al. 1995 *Phys. Plasmas* **2** in press.

[167] Tamano T 1995 *Phys. Plasmas* **2** in press.

[168] Sakai O, Yasaka Y, Itatani R 1993 *Phys. Rev. Lett.* **70** 4071.

[169] Itoh S-I, Itoh K 1990 *Comments Plasma Phys. Contr. Fusion* **13** 141.

[170] Catto P J, Hazeltine R D 1994 *Phys. Plasmas* **1** 1882.

Catto P J, Connor J W 1995 *Phys. Plasmas* **2** 218.

[171] Lichtenberg A J, Liebermann M A 1984 *Regular and Stochastic Motion* (Springer Verlag, New York).

[172] Callen J D 1977 *Phys. Rev. Lett.* **39** 1540.

[173] Kubota T, Itoh S-I, Toda S, Yamaguchi H, Fukuyama A 1995 *Trans. Fusion Tech.* **27** 493.

[174] Toi K et al 1990 *Phys. Rev. Lett.* **64** 1895.

[175] Kadomtsev B B 1992 *Tokamak Plasma: a complex physical system* (IOP Publishing, Bristol).

Figure Captions

Fig.1 Conceptual diagram of this review article. In the beginning, the effects of radial electric field on the particle orbit and the collisional transport are presented. Next the influence of the electric field on the anomalous transport is discussed. Then the generation mechanism of the radial electric field is explained. Based on these processes, the evolution of the plasma and electric field structure is investigated.

Fig.2 Geometry and coordinates. In the toroidal model, the coordinates (R, ζ, Z) and (r,θ,ζ) are used. In the cylindrical model or the slab model, coordinates (r,θ,z) or (x,y,z) are used, respectively.

Fig.3 Schematic drawing of the ripple trapped particles in tokamaks (a) and in helical systems (b). In (a), discrete toroidal coils produce the variation of |B| in the ζ-direction. The particles trapped in the local mirror drift in the vertical direction. In (b), helically-trapped particles drift along the helical pitch of the system. The projection in the poloidal cross-section (c) illustrates the drift surface of the center of the helically-trapped particles (thin solid line) and the magnetic surface (dotted line).

Fig.4 Distinction of the transit particles and banana particles in tokamaks is shown in the velocity space in the rotating coordinate. Shaded area indicates the particles touching the limiter.

Fig.5 The loss cone region for the particles which are deeply trapped in the helical ripple is shown in the r/a-W plane (shaded region). Boundaries of the region are expressed by W_+ and W_-. (r/a =1 shows the edge at the low-field-side and r/a = -1 denotes that at the high-field side.)

Fig.6 The velocity shear (a). The circular element (diameter L) at t = 0 is stretched after the elapse of time t = t :(b). In the latter time, the longer length of the ellipse is given as $L_{\parallel} = L\sqrt{1 + S_v^2 t^2}$, and the shorter axis is given by $L_{\perp} = (1 + S_v^2 t^2)^{-1/2} L$.

Fig.7 Structure factor S(k) of fluctuations in the fluid dynamics. The solid line is the case with the flow shear, and the dashed line is the case without. The reduction is prominent for the longer-wave-length region.

Fig.8 Mode growth rate as a function of the fluctuation level (turbulent driven transport coefficient). The thick solid line shows the case of self-sustained turbulence. Dotted line indicates the picture of the Kadomtsev formula. In the self-sustained turbulence, high saturation level is possible independent of the linear stability.

Fig.9 Flow pattern is twisted and the mirror-invariance is not satisfied. (There is a phase relation between $\tilde{V}_y$ and $\tilde{V}_x$ such that the x-component of the fluctuating velocity is positive when the y-component is positive.) In this case, the poloidal momentum (in the y-direction) is transported in the x-direction (i.e., radial direction).

Fig.10 Relation between gradient and flux. Hard transition model (a) and soft transition model (b). The cusp-type bifurcation with hard transition is summarized in (c).

Fig.11 Schematic relation between the plasma parameter (g) and the diffusivity (i.e., the flux divided by the gradient). The dotted line indicate the hysteresis and the limit cycles.

Fig.12 Examples of the electric field bifurcation. In (a), the balance between $\Gamma_{e\text{-}i}^{anom}$ and the loss cone loss is shown. The self-consistent flux, as a function of the gradient,

is shown in (b). In (c) another example, i.e., the balance between the loss cone loss (solid line) and Γ^{bv} (dashed line), is demonstrated.

Fig.13 Flow pattern induced by the poloidal flow. The picture in the neoclassical theory is given in (a). The poloidal flow is associated with the flow along the field line. The flow along the field line changes its sign in the outside and in the inside of the torus,respectively. Alternative way to satisfy the divergence-free condition is given in (b). In the edge region, where the sharp radial gradient exists, small amount of the $\sin\theta$-dependent radial flow compensates the compression in the poloidal direction. The return flow is denoted by the dotted line.

Fig.14 Formation of the *meso phase* in the presence of the viscosity for the media which allows the bifurcation. Thin solid line indicates the solution of the local equation, that allows the multiple states X_u and X_l. As the parameter g gradually changes in space, the upper branch and lower branch are connected at the location of $g = g_*$. Due to the finite viscosity, the interface layer has the finite width, the solution in which is shown by the thick solid line. In this layer, the solution X takes the intermediate value between X_u and X_l, and this region is called as the meso phase.

Fig.15 Poloidal shock formation is expressed in the poloidal variation of the static potential (a). The poloidal variation of $e\tilde{\phi}_0/T_e$ is shown for the case of $|M_p - 1| < \sqrt{\varepsilon}$. (The vertical axis is shifted by a number which is $O(\sqrt{\varepsilon})$. Quoted from [89].) The radial component of the $E \times B$ velocity associated with this potential variation is shown schematically in (b).

Fig.16 Contour of the thermal transport coefficient χ as a function of the pressure gradient (α) and the electric field inhomogeneity (ω_{E1}). In the absence of the electric field shear, E_r', the higher the pressure gradient, the larger the thermal conductivity is. (This feature is the origin of the power degradation in the L-mode confinement.)

Fig.17 Establishment of the transport barrier near the edge. The spatial structure of the effective diffusivity (i.e., the ratio of the flux to the gradient) is shown by the solid line and dashed line in the H-state and L-state, respectively.

Fig.18 Periodic formation and destruction of the edge transport barrier give rise to the periodic bursts of the outflow. Note that the supply from the core is constant in time. (Quoted from [83].)

Fig.19 Gradual change of the heating power causes the sudden transitions from L-to ELMy state and from ELMy to ELM-free-H state. Note that the amplitude of the first burst is almost equal to the second and that the last one is similar to preceding ones. Details of the shape of the bursts tell the difference between the shapes of the bursts in the beginning phase and ending phase. (Quoted from [93].)

Fig.20 Transient response of the transport barrier. A local enhancement of D is made in the region of $-2 < x, -1$ and $5 < t < 6$ to simulate the violent dynamics just inside of the transport barrier. (See [92] for the normalization of x and t.).

Fig.21 Transport simulation of the density peaking by the CNTR-NBI (for the parameters of JFT-2M tokamak). Temporal evolution of the peaking factor is shown in (a) and the radial profile is given in (b). (Quoted from [129].)

Fig.22 Transport simulation of the VH-mode formation. In (a), the temporal evolution of the profiles predicted by the model of [104] is quoted: In the very beginning, the H-transition occurs; somewhar later, the transport barrier width increases. In (b), the model of [132] is quoted. The interaction between the improved confinement and Bootstrap current generation allows the well-like reduction of the thermal conductivity and the improved confinement in the core.

Fig.1

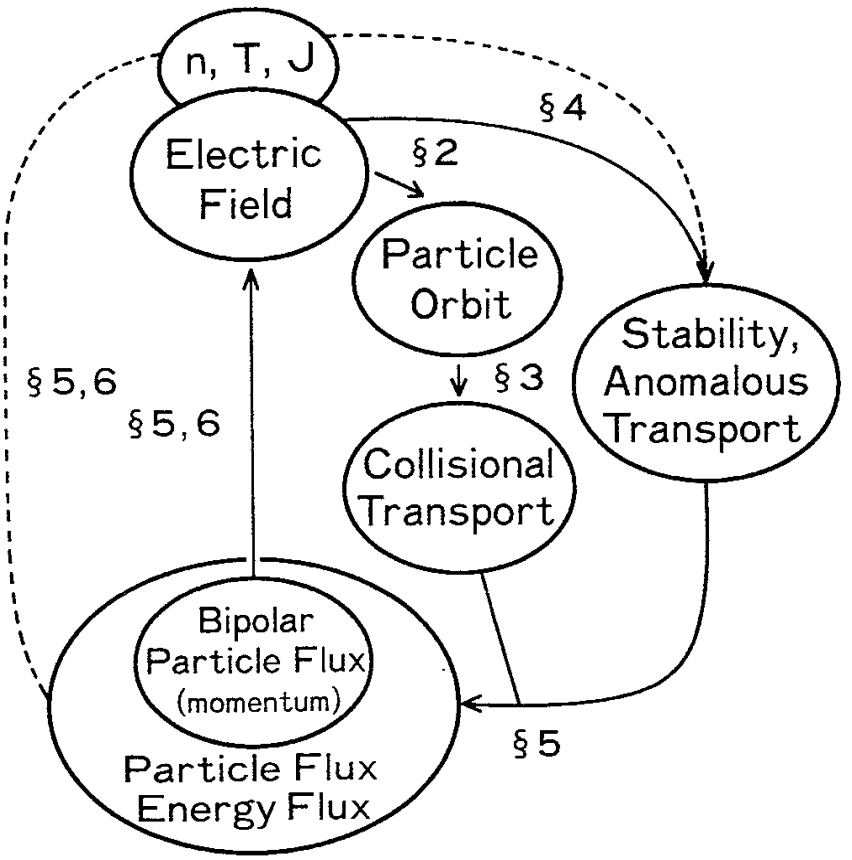
n, T, J
§4
Electric Field
§2
Particle Orbit
Stability, Anomalous Transport
§5,6
§5,6
§3
Collisional Transport
Bipolar Particle Flux (momentum)
Particle Flux Energy Flux
§5

Fig.2

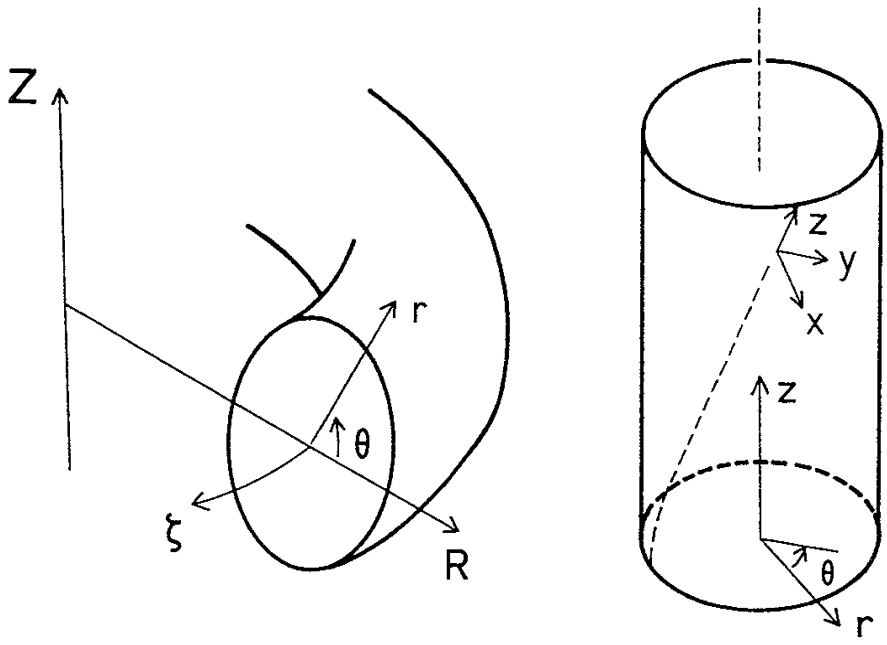

Fig.3

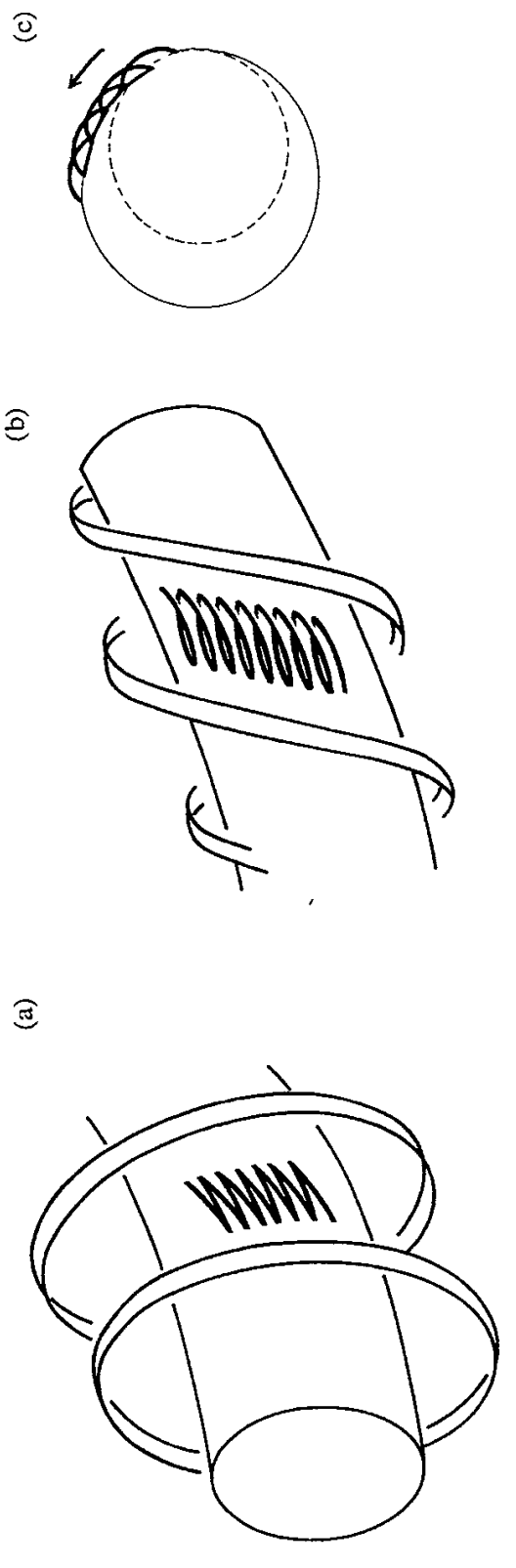

Fig.4

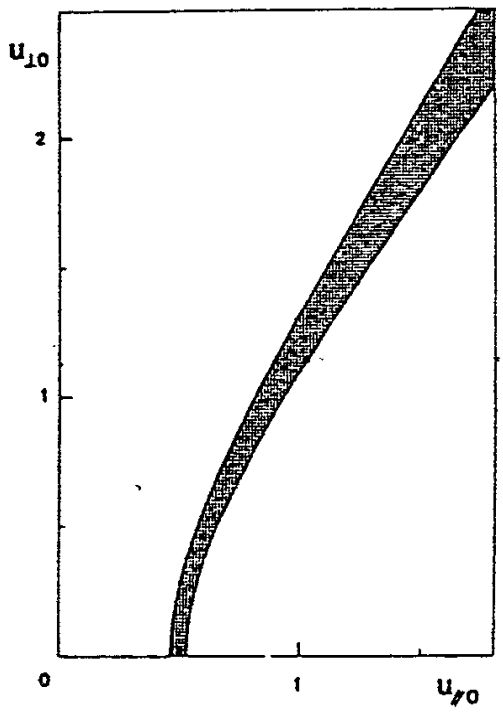

Fig.5

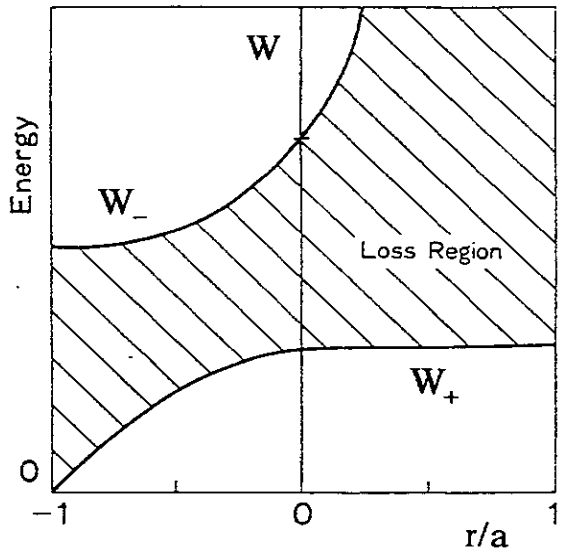

Fig.6

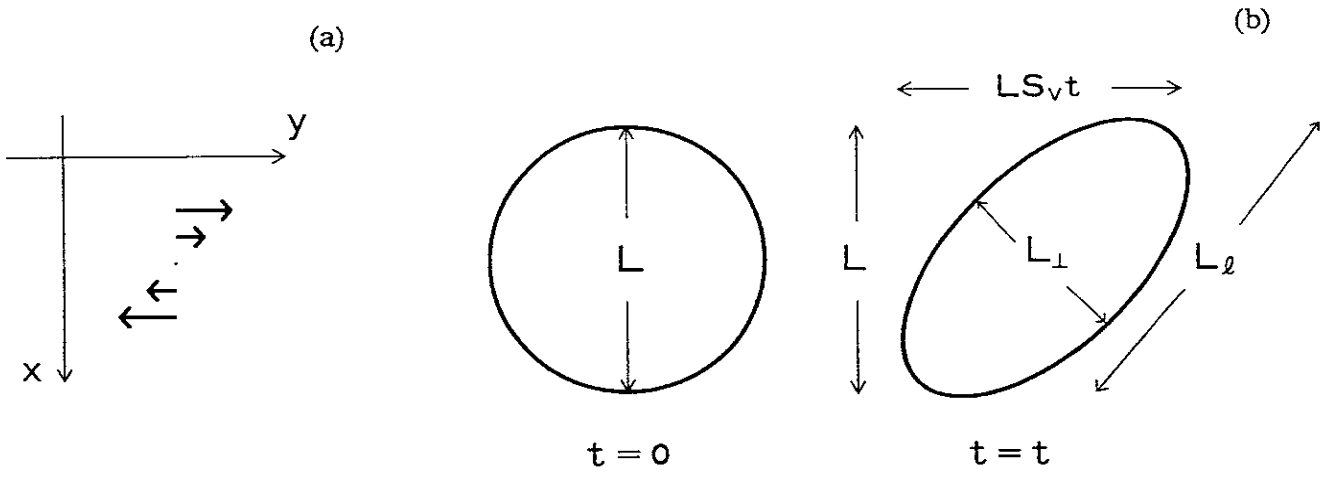

Fig.7

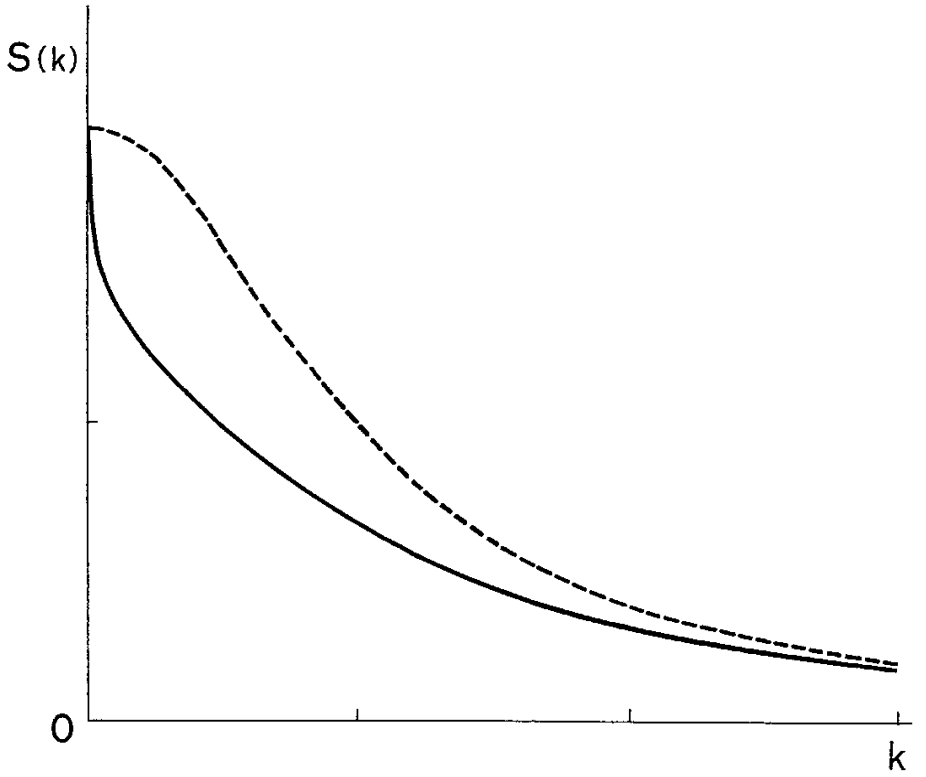

Fig.8

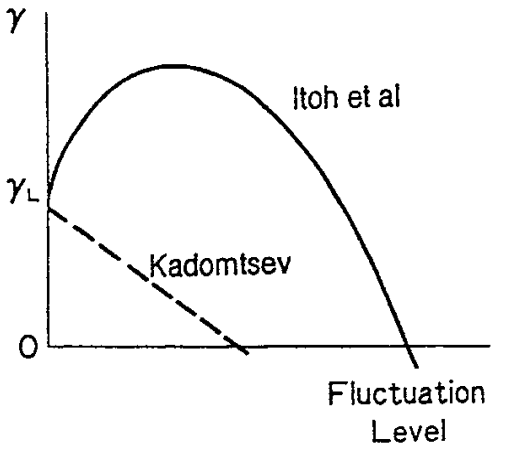

Fig.9

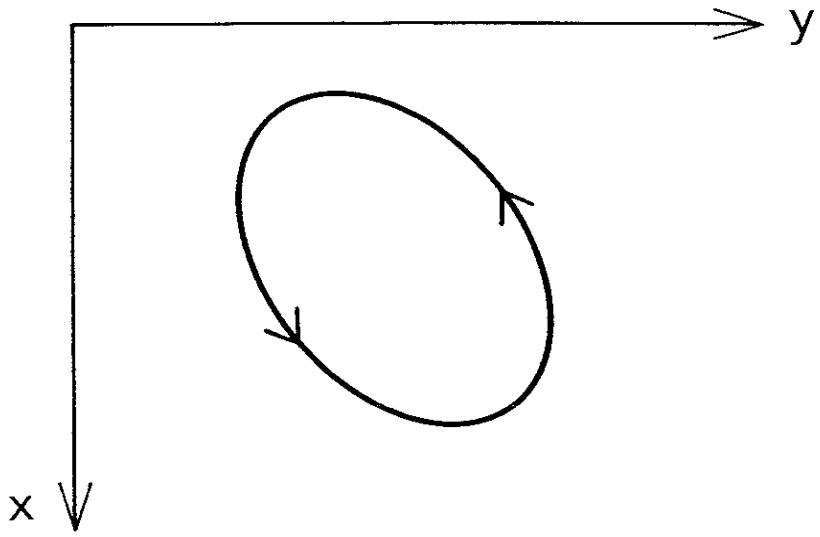

Fig.10

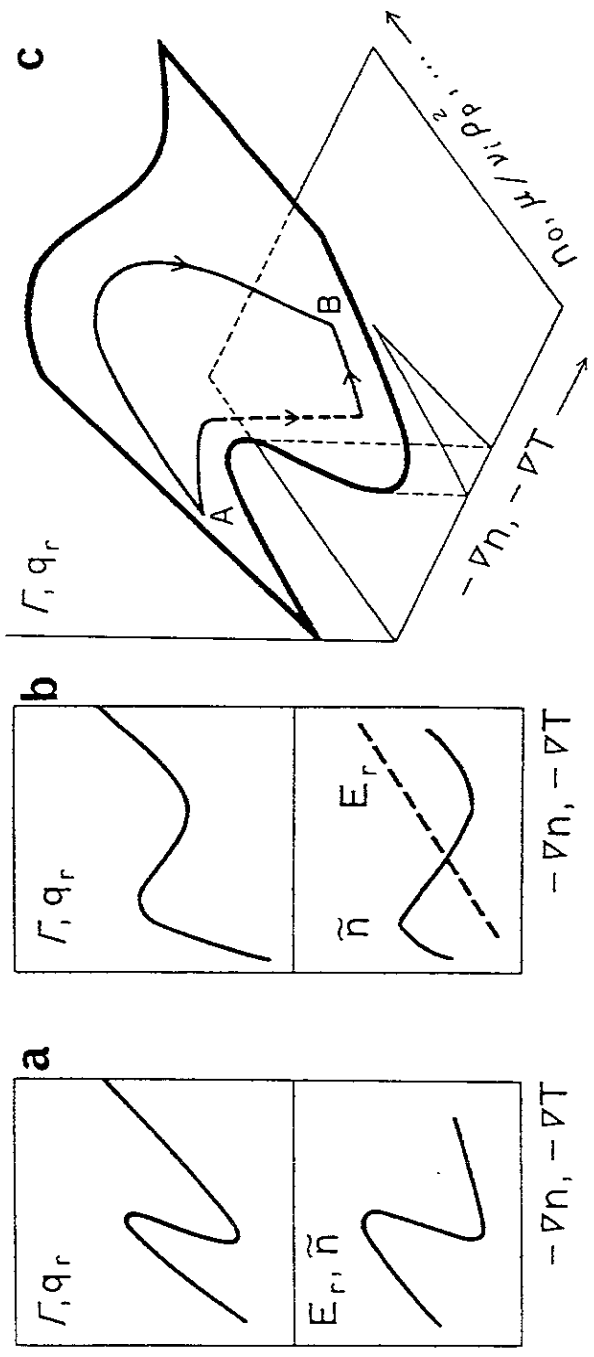

Fig.11

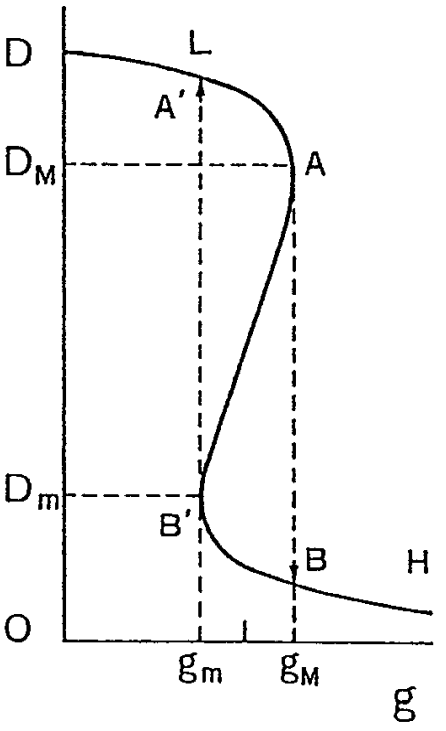

Fig.12

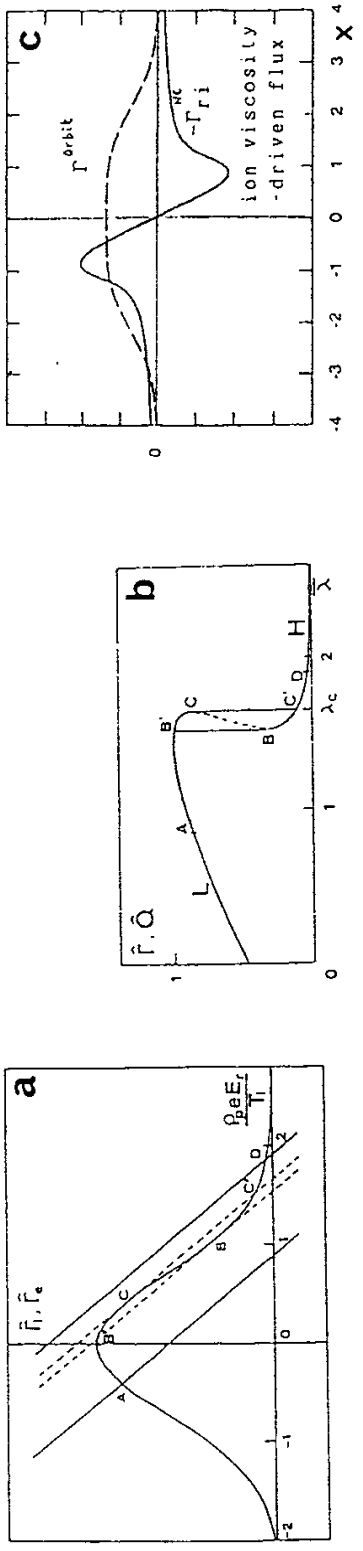

Fig.13

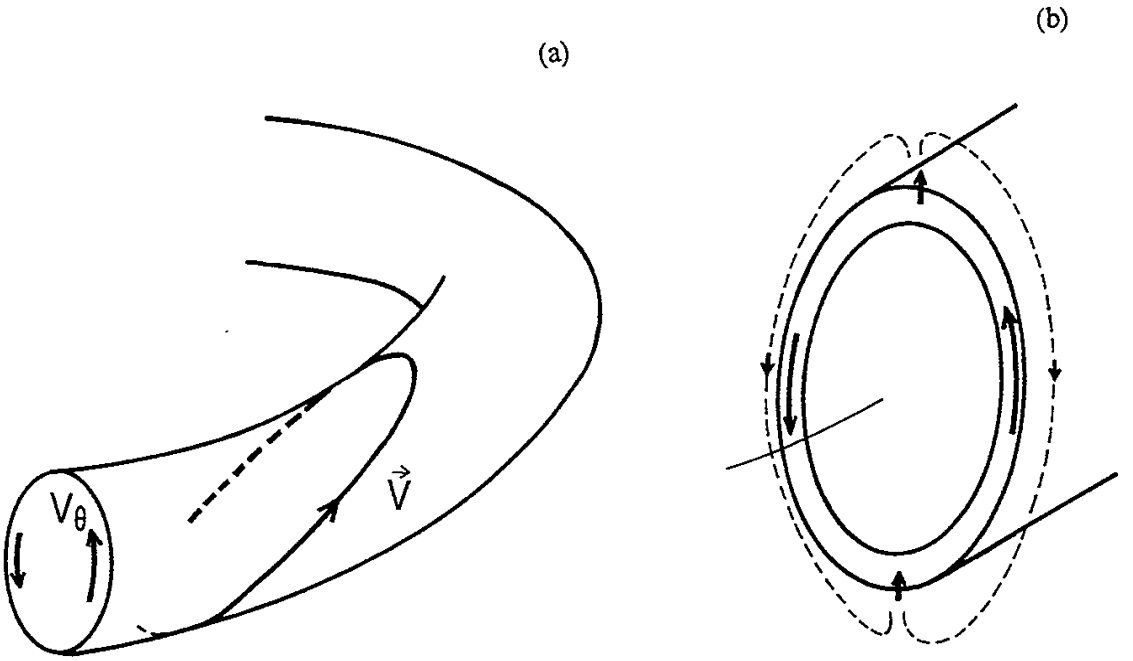

Fig.14

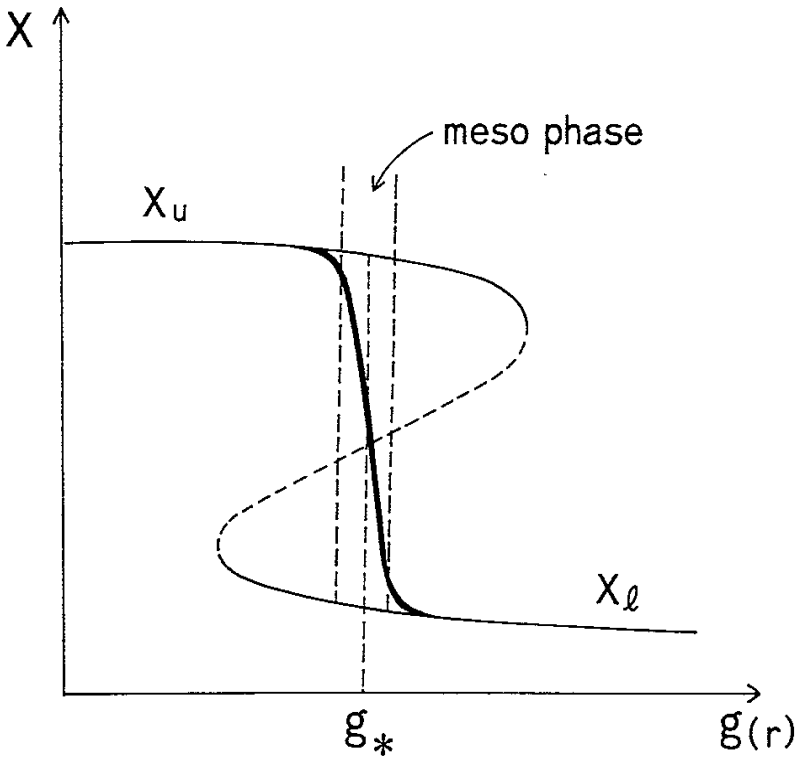

Fig.15

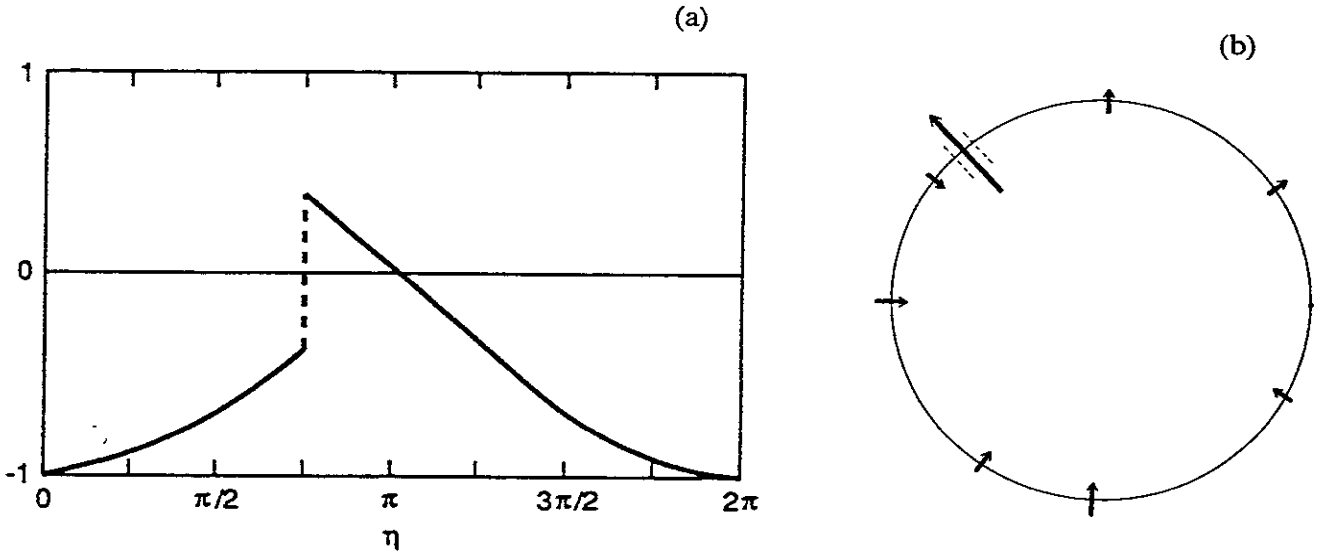

Fig.16

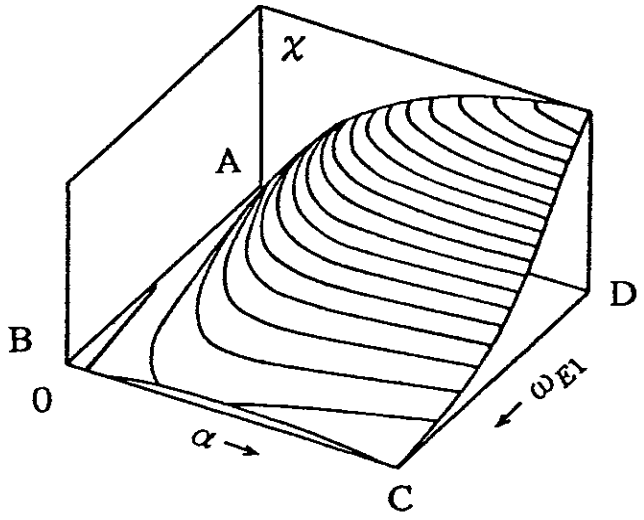

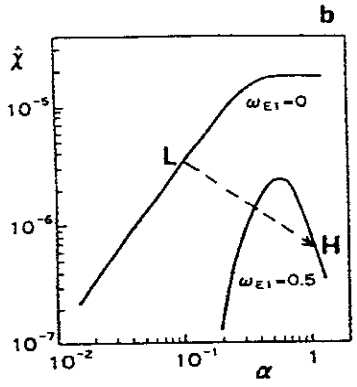

Fig.17

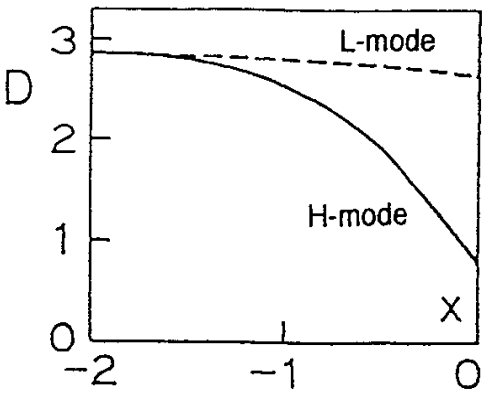

Fig.18

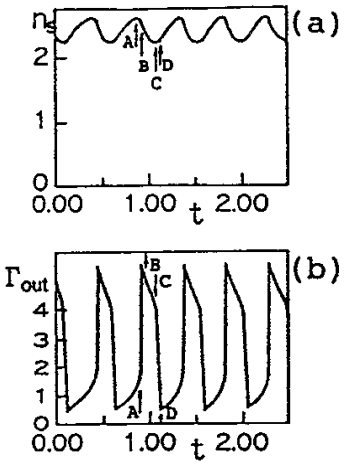

Fig.19

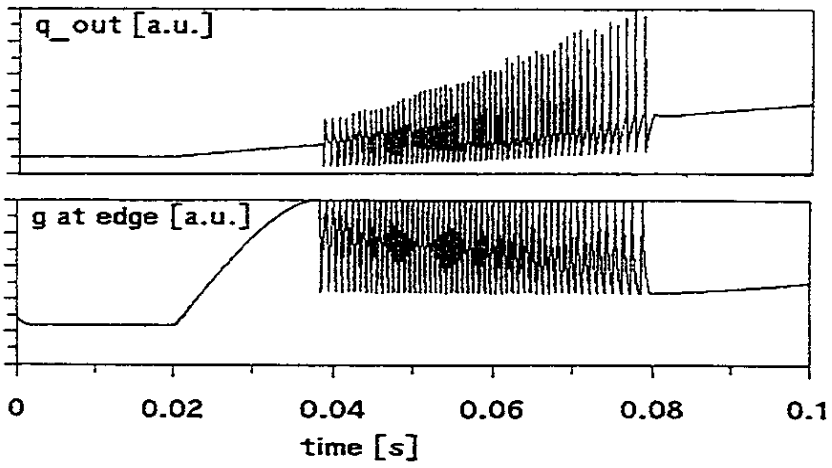

Fig.20

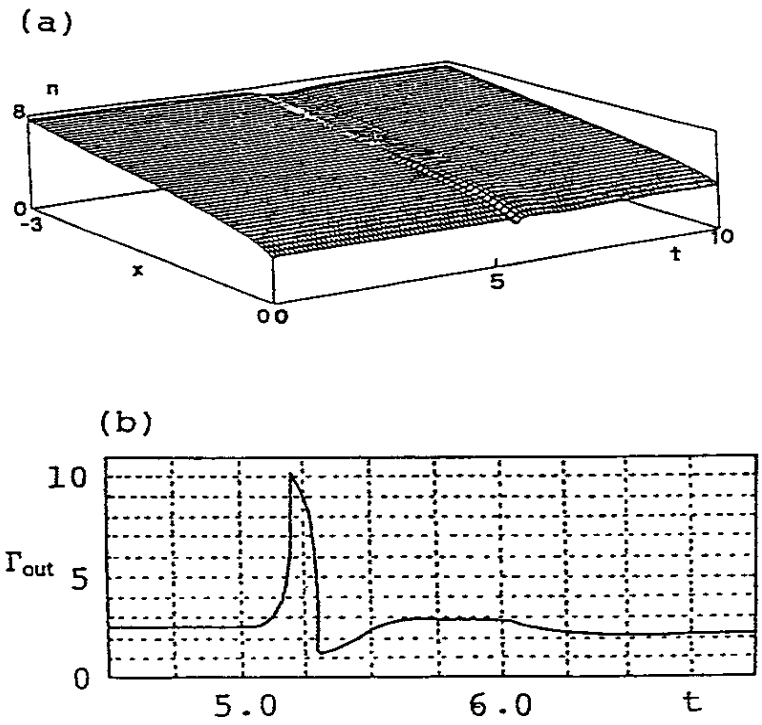

Fig.21

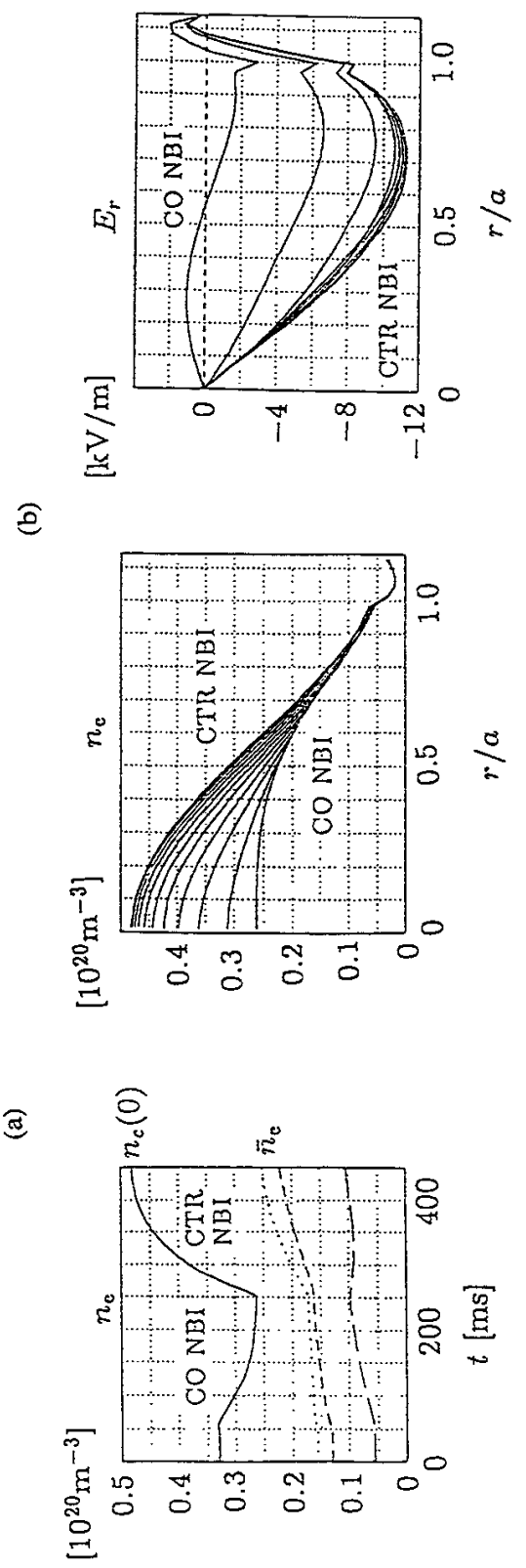
(a)
$[10^{20}m^{-3}]$
n_e
$n_e(0)$
$\bar{n}_e$
CO NBI
CTR NBI
0.5
0.4
0.3
0.2
0.1
0
0
200
400
t [ms]
(b)
$[10^{20}m^{-3}]$
n_e
CTR NBI
CO NBI
0.4
0.3
0.2
0.1
0
0
0.5
1.0
r/a
[kV/m]
E_r
CO NBI
CTR NBI
0
−4
−8
−12
0
0.5
1.0
r/a

Fig.22 (a)

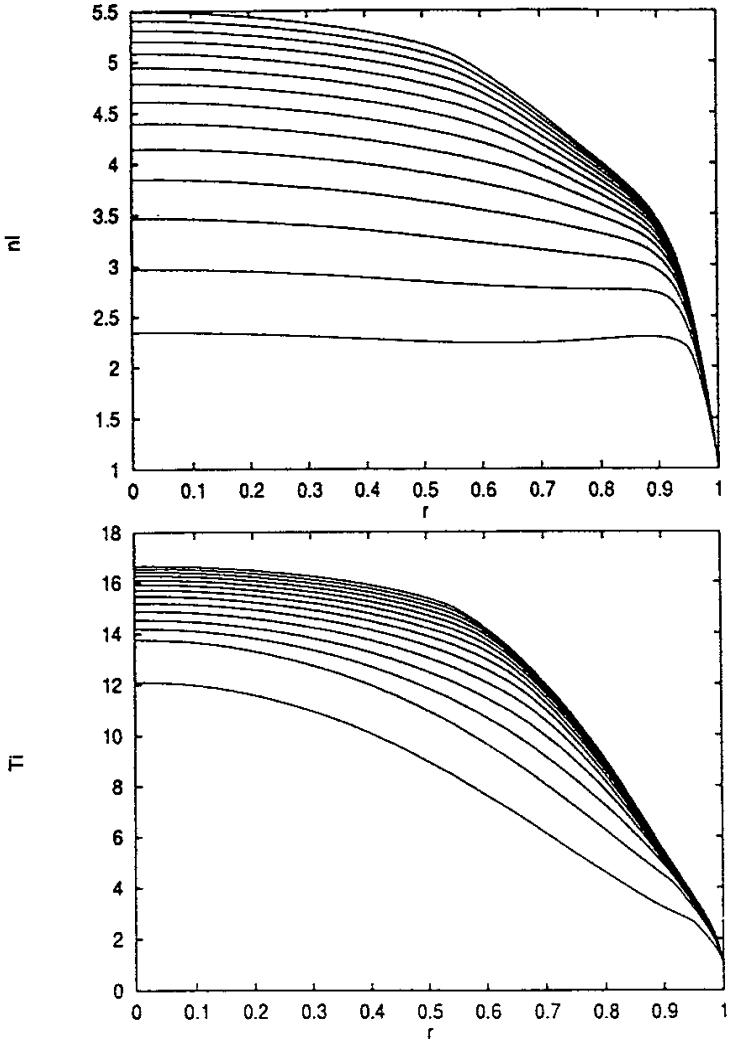
ni
5.5
5
4.5
4
3.5
3
2.5
2
1.5
1
0
0.1
0.2
0.3
0.4
0.5
0.6
0.7
0.8
0.9
1
r
Ti
18
16
14
12
10
8
6
4
2
0
0
0.1
0.2
0.3
0.4
0.5
0.6
0.7
0.8
0.9
1
r

Fig.22 (b)

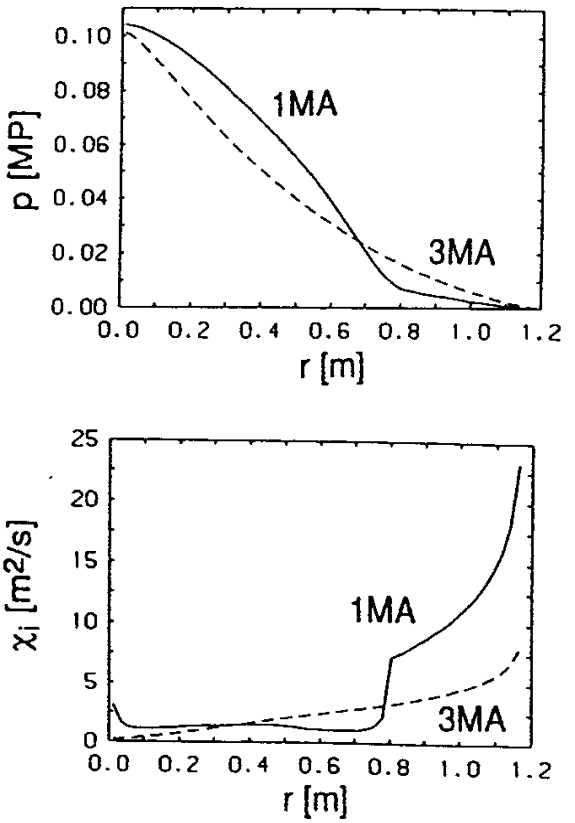
0.10
0.08
0.06
0.04
0.02
0.00
p [MP]
1MA
3MA
0.0
0.2
0.4
0.6
0.8
1.0
1.2
r [m]
25
20
15
10
5
0
χi [m2/s]
1MA
3MA
0.0
0.2
0.4
0.6
0.8
1.0
1.2
r [m]

Recent Issues of NIFS Series

NIFS-317 A. Fujisawa, H. Iguchi, M. Sasao and Y. Hamada,
Second Order Focusing Property of 210° Cylindrical Energy Analyzer;
Nov. 1994

NIFS-318 T. Sato and Complexity Simulation Group,
Complexity in Plasma - A Grand View of Self- Organization; Nov. 1994

NIFS-319 Y. Todo, T. Sato, K. Watanabe, T.H. Watanabe and R. Horiuchi,
MHD-Vlasov Simulation of the Toroidal Alfvén Eigenmode; Nov. 1994

NIFS-320 A. Kageyama, T. Sato and The Complexity Simulation Group,
Computer Simulation of a Magnetohydrodynamic Dynamo II: Nov. 1994

NIFS-321 A. Bhattacharjee, T. Hayashi, C.C.Hegna, N. Nakajima and T. Sato,
Theory of Pressure-induced Islands and Self-healing in Three-dimensional Toroidal Magnetohydrodynamic Equilibria; Nov. 1994

NIFS-322 A. Iiyoshi, K. Yamazaki and the LHD Group,
Recent Studies of the Large Helical Device; Nov. 1994

NIFS-323 A. Iiyoshi and K. Yamazaki,
The Next Large Helical Devices; Nov. 1994

NIFS-324 V.D. Pustovitov
Quasisymmetry Equations for Conventional Stellarators; Nov. 1994

NIFS-325 A. Taniike, M. Sasao, Y. Hamada, J. Fujita, M. Wada,
The Energy Broadening Resulting from Electron Stripping Process of a Low Energy Au^- Beam; Dec. 1994

NIFS-326 I. Viniar and S. Sudo,
New Pellet Production and Acceleration Technologies for High Speed Pellet Injection System "HIPEL" in Large Helical Device; Dec. 1994

NIFS-327 Y. Hamada, A. Nishizawa, Y. Kawasumi, K. Kawahata, K. Itoh, A. Ejiri, K. Toi, K. Narihara, K. Sato, T. Seki, H. Iguchi, A. Fujisawa, K. Adachi, S. Hidekuma, S. Hirokura, K. Ida, M. Kojima, J. Koong, R. Kumazawa, H. Kuramoto, R. Liang, T. Minami, H. Sakakita, M. Sasao, K.N. Sato, T. Tsuzuki, J. Xu, I. Yamada, T. Watari,
Fast Potential Change in Sawteeth in JIPP T-IIU Tokamak Plasmas;
Dec. 1994

NIFS-328 V.D. Pustovitov,
Effect of Satellite Helical Harmonics on the Stellarator Configuration;
Dec. 1994

NIFS-329 K. Itoh, S-I. Itoh and A. Fukuyama、
A Model of Sawtooth Based on the Transport Catastrophe; Dec. 1994

NIFS-330 K. Nagasaki, A. Ejiri,
Launching Conditions for Electron Cyclotron Heating in a Sheared Magnetic Field; Jan. 1995

NIFS-331 T.H. Watanabe, Y. Todo, R. Horiuchi, K. Watanabe, T. Sato,
An Advanced Electrostatic Particle Simulation Algorithm for Implicit Time Integration; Jan. 1995

NIFS-332 N. Bekki and T. Karakisawa,
Bifurcations from Periodic Solution in a Simplified Model of Two-dimensional Magnetoconvection; Jan. 1995

NIFS-333 K. Itoh, S.-I. Itoh, M. Yagi, A. Fukuyama,
Theory of Anomalous Transport in Reverse Field Pinch; Jan. 1995

NIFS-334 K. Nagasaki, A. Isayama and A. Ejiri
Application of Grating Polarizer to 106.4GHz ECH System on Heliotron-E; Jan. 1995

NIFS-335 H. Takamaru, T. Sato, R. Horiuchi, K. Watanabe and Complexity Simulation Group,
A Self-Consistent Open Boundary Model for Particle Simulation in Plasmas; Feb. 1995

NIFS-336 B.B. Kadomtsev,
Quantum Telegragh : is it possible?; Feb. 1995

NIFS-337 B.B.Kadomtsev,
Ball Lightning as Self-Organization Phenomenon; Feb. 1995

NIFS-338 Y. Takeiri, A. Ando, O. Kaneko, Y. Oka, K. Tsumori, R. Akiyama, E. Asano, T. Kawamoto, M. Tanaka and T. Kuroda,
High-Energy Acceleration of an Intense Negative Ion Beam; Feb. 1995

NIFS-339 K. Toi, T. Morisaki, S. Sakakibara, S. Ohdachi, T.Minami, S. Morita, H. Yamada, K. Tanaka, K. Ida, S. Okamura, A. Ejiri, H. Iguchi, K. Nishimura, K. Matsuoka, A. Ando, J. Xu, I. Yamada, K. Narihara, R. Akiyama, H. Idei, S. Kubo, T. Ozaki, C. Takahashi, K. Tsumori,
H-Mode Study in CHS; Feb. 1995

NIFS-340 T. Okada and H. Tazawa,
Filamentation Instability in a Light Ion Beam-plasma System with External Magnetic Field; Feb. 1995

NIFS-341 T. Watanbe, G. Gnudi,
A New Algorithm for Differential-Algebraic Equations Based on HIDM;

Feb. 13, 1995

NIFS-342 Y. Nejoh,
New Stationary Solutions of the Nonlinear Drift Wave Equation;
Feb. 1995

NIFS-343 A. Ejiri, S. Sakakibara and K. Kawahata,
Signal Based Mixing Analysis for the Magnetohydrodynamic Mode Reconstruction from Homodyne Microwave Reflectometry; Mar.. 1995

NIFS-344 B.B.Kadomtsev, K. Itoh, S.-I. Itoh
Fast Change in Core Transport after L-H Transition; Mar. 1995

NIFS-345 W.X. Wang, M. Okamoto, N. Nakajima and S. Murakami,
An Accurate Nonlinear Monte Carlo Collision Operator; Mar. 1995

NIFS-346 S. Sasaki, S. Takamura, S. Masuzaki, S. Watanabe, T. Kato, K. Kadota,
Helium I Line Intensity Ratios in a Plasma for the Diagnostics of Fusion Edge Plasmas; Mar. 1995

NIFS-347 M. Osakabe,
Measurement of Neutron Energy on D-T Fusion Plasma Experiments;
Apr. 1995

NIFS-348 M. Sita Janaki, M.R. Gupta and Brahmananda Dasgupta,
Adiabatic Electron Acceleration in a Cnoidal Wave; Apr. 1995

NIFS-349 J. Xu, K. Ida and J. Fujita,
A Note for Pitch Angle Measurement of Magnetic Field in a Toroidal Plasma Using Motional Stark Effect; Apr. 1995

NIFS-350 J. Uramoto,
Characteristics for Metal Plate Penetration of a Low Energy Negative Muonlike or Pionlike Particle Beam: Apr. 1995

NIFS-351 J. Uramoto,
An Estimation of Life Time for A Low Energy Negative Pionlike Particle Beam: Apr. 1995

NIFS-352 A. Taniike,
Energy Loss Mechanism of a Gold Ion Beam on a Tandem Acceleration System: May 1995

NIFS-353 A. Nishizawa, Y. Hamada, Y. Kawasumi and H. Iguchi,
Increase of Lifetime of Thallium Zeolite Ion Source for Single-Ended Accelerator: May 1995

NIFS-354 S. Murakami, N. Nakajima, S. Okamura and M. Okamoto,
Orbital Aspects of Reachable β Value in NBI Heated

Heliotron/Torsatrons; May 1995

NIFS-355 H. Sugama and W. Horton,
Neoclassical and Anomalous Transport in Axisymmetric Toroidal Plasmas with Electrostatic Turbulence; May 1995

NIFS-356 N. Ohyabu
A New Boundary Control Scheme for Simultaneous Achievement of H-mode and Radiative Cooling (SHC Boundary); May 1995

NIFS-357 Y. Hamada, K.N. Sato, H. Sakakita, A. Nishizawa, Y. Kawasumi, R. Liang, K. Kawahata, A. Ejiri, K. Toi, K. Narihara, K. Sato, T. Seki, H. Iguchi, A. Fujisawa, K. Adachi, S. Hidekuma, S. Hirokura, K. Ida, M. Kojima, J. Koong, R. Kumazawa, H. Kuramoto, T. Minami,. M. Sasao, T. Tsuzuki, J.Xu, I. Yamada, and T. Watari,
Large Potential Change Induced by Pellet Injection in JIPP T-IIU Tokamak Plasmas; May 1995

NIFS-358 M. Ida and T. Yabe,
Implicit CIP (Cubic-Interpolated Propagation) Method in One Dimension; May 1995

NIFS-359 A. Kageyama, T. Sato and The Complexity Simulation Group,
Computer Has Solved A Historical Puzzle: Generation of Earth's Dipole Field; June 1995

NIFS-360 K. Itoh, S.-I. Itoh, M. Yagi and A. Fukuyama,
Dynamic Structure in Self-Sustained Turbulence; June 1995

NIFS-361 K. Kamada, H. Kinoshita and H. Takahashi,
Anomalous Heat Evolution of Deuteron Implanted Al on Electron Bombardment; June 1995

NIFS-362 V.D. Pustovitov,
Suppression of Pfirsch-schlüter Current by Vertical Magnetic Field in Stellarators; June 1995

NIFS-363 A. Ida, H. Sanuki and J. Todoroki
An Extended K-dV Equation for Nonlinear Magnetosonic Wave in a Multi-Ion Plasma; June 1995

NIFS-364 H. Sugama and W. Horton
Entropy Production and Onsager Symmetry in Neoclassical Transport Processes of Toroidal Plasmas; July 1995

NIFS-365 K. Itoh, S.-I. Itoh, A. Fukuyama and M. Yagi,
On the Minimum Circulating Power of Steady State Tokamaks; July 1995